(2)

NAVAL POSTGRADUATE SCHOOL
Monterey, California

THESIS

A MODEL ANALYSIS OF POTENTIAL VORTICITY ON
ISOPYCNAL SURFACES
FOR THE GLOBAL OCEAN

by

Douglas Craig Marble

September, 1993

Thesis Advisor: Albert J. Semtner

Approved for public release; distribution is unlimited.

REPORT DOCUMENTATION PAGE

Form Approved OMB No. 0704

1. AGENCY USE ONLY *(Leave blank)*	2. REPORT DATE	3. REPORT TYPE AND DATES COVERED
	September, 1993	Master's Thesis

4. TITLE AND SUBTITLE **A Model Analysis of Potential Vorticity on Isopycnal Surfaces for the Global Ocean**

5. FUNDING NUMBERS

6. AUTHOR(S) **Douglas Craig Marble**

7. PERFORMING ORGANIZATION NAME(S) AND ADDRESS(ES)
Naval Postgraduate School
Monterey CA 93943-5000

8. PERFORMING ORGANIZATION REPORT NUMBER

9. SPONSORING/MONITORING AGENCY NAME(S) AND ADDRESS(ES)

10. SPONSORING/ MONITORING AGENCY REPORT NUMBER

11. SUPPLEMENTARY NOTES **The views expressed in this thesis are those of the author and do not reflect the official policy or position of the Department of Defense or the U.S. Government.**

12a. DISTRIBUTION/AVAILABILITY STATEMENT
Approved for public release; distribution is unlimited.

12b. DISTRIBUTION CODE
A

13. ABSTRACT *(maximum 200 words)*

Charts of potential vorticity (q) within four different density layers, calculated from an eddy resolving global ocean general circulation model, are presented for the Atlantic, Pacific, and Indian Ocean Basins. Potential Vorticity is evaluated as $q = (f/\rho)*(\Delta\sigma/\Delta z)$, a formulation that is valid for large, slow scales and allows it to be readily calculated from model output. Here, f is Coriolis, ρ in situ density, σ the potential density referred to the sea surface, and z the vertical coordinate.

The model is shown to represent oceanic density structure with reasonable accuracy. The most significant departure from observations are the steep density gradients on the northern boundary of the Antarctic Circumpolar Current. This may be due to model convective adjustment parameterizations and the extent of the smoothing in the cataloged data, which may be greater in the southern oceans due to relatively scarce observations. Model derived values of potential vorticity correspond well with those calculated from observations. In the middle and lower layers, the three basins tend toward homogenization, representing unventilated layers. "Gyres" of q in the upper layers of the northern Atlantic and Pacific Oceans, with their northern boundaries anchored in the outcrop region, illustrate the ventilation of these layers.

14. SUBJECT TERMS **Oceanography, Numercial Modeling, Potential Vorticity.**

15. NUMBER OF PAGES **81**

16. PRICE CODE

17. SECURITY CLASSIFICATION OF REPORT	18. SECURITY CLASSIFICATION OF THIS PAGE	19. SECURITY CLASSIFICATION OF ABSTRACT	20. LIMITATION OF ABSTRACT
Unclassified	**Unclassified**	**Unclassified**	**UL**

NSN 7540-01-280-5500

Standard Form 298 (Rev. 2-89)
Prescribed by ANSI Std. 239-18

Approved for public release; distribution is unlimited.

A Model Analysis of Potential Vorticity on Isopycnal Surfaces for the Global Ocean

by

Douglas Craig Marble
Lieutenant, United States Navy
B.S., University of South Carolina, 1986

Submitted in partial fulfillment of the requirements for the degree of

MASTER OF SCIENCE IN METEOROLOGY AND PHYSICAL OCEANOGRAPHY

from the

NAVAL POSTGRADUATE SCHOOL
September, 1993

Author: _____
Douglas Craig Marble

Approved By: _____
Albert J. Semtner, Thesis Advisor

_____
Mary L. Batteen, Second Reader

_____
Curtis A. Collins, Chairman, Department of Oceanography

ABSTRACT

Charts of potential vorticity (q) within four different density layers, calculated from an eddy resolving global ocean general circulation model, are presented for the Atlantic, Pacific, and Indian Ocean Basins. Potential vorticity is evaluated as $q = (f/\rho)*(\Delta\sigma/\Delta z)$, a formulation that is valid for large, slow scales and allows it to be readily calculated from model output. Here, f is Coriolis, ρ in situ density, σ the potential density referred to the sea surface, and z the vertical coordinate.

The model is shown to represent oceanic density structure with reasonable accuracy. The most significant departure from observations are the steep density gradients on the northern boundary of the Antarctic Circumpolar Current (ACC). This may be due to model convective adjustment parameterizations and the extent of the smoothing in the cataloged data, which may be greater in the southern oceans due to relatively scarce observations. Model derived values of potential vorticity correspond well with those calculated from observations. In the middle and lower layers, the three basins tend toward homogenization, representing unventilated layers. "Gyres" of q in the upper layers of the northern Atlantic and Pacific Oceans, with their northern boundaries anchored in the outcrop region, illustrate the ventilation of these layers.

TABLE OF CONTENTS

I. INTRODUCTION

Several theories attempt to predict the horizontal and vertical structure of the thermocline (e.g., Rhines and Young, 1982; Luyten *et al.*, 1983; Pedlosky and Young, 1983; Pedlosky, 1983). These theories all revolve around the role of potential vorticity (q). Potential vorticity is a calculated oceanic property that is conservative in the absence of processes which change water parcel characteristics, such as turbulent mixing or surface forcing. It can be considered a measure similar to potential angular momentum induced by Coriolis and other forces affecting water properties, as reflected primarily in changes in density gradients.

The Ertel potential vorticity is the total vorticity (the sum of Coriolis and relative vorticity) times the gradient of density, divided by the density. For most of the ocean, the strongest density gradients are in the vertical, so potential vorticity is approximately the total vorticity times the vertical gradient of density, divided by density.

A final approximation is that the relative vorticity is small compared to Coriolis (assuming a small Rossby number) so relative vorticity can be eliminated. Calculations of relative vorticity from model output support this

approximation. McDowell, et al. (1982) defined potential vorticity as $q = (f/\rho)*d(\rho)/dz$. Where f is Coriolis, ρ in situ density, and z is the vertical coordinate. In isopycnal coordinates, the density gradient is represented by the distance between density surfaces rather than the density change between pressure (depth) surfaces. For large scale, quasi-geostrophic flows, relative vorticity is much smaller than the vortex stretching part of q, and so, to predict the field of potential vorticity is to predict the vertical separation between density surfaces. Determining the vertical structure of the global thermocline hinges around this problem.

The objective of this study is to calculate model fields of potential vorticity from the Semtner and Chervin (1988, 1992) global ocean circulation model and compare them to observed potential vorticity fields. This will indicate the character of the model ocean's thermocline and the accuracy of its portrayal of the observed thermocline, as determined from the Levitus (1982) data. The intention is to see where the model is successful in correctly predicting potential vorticity distribution and to see where it fails. In particular, model results will be compared with the work of Keffer (1985) and his treatment of the "directly ventilated" theory of Luyten *et al.* (1983) and the "unventilated" theory of Rhines and Young (1982a). While these theories predict fluid properties as they propagate

along isopycnal layers, they differ in the degree to which they consider the layer to be isolated from surface boundary conditions.

The degree of exposure to surface boundary conditions and forcing will determine the characteristics of a layer within the subtropical gyre thermocline. The potential vorticity of fluid particles recirculating within ventilated layers is reset with each circuit around the gyre, as the particles pass through the outcrop zone. This outcropping of density layers allows deep vertical motion to be forced by Ekman pumping, resulting in deep ventilation, which advects to latitudes far south of the outcrop where the layer is shielded from direct wind influence. Particles within unventilated layers remain isolated from surface conditions long enough to approach a common homogenized state, sharing their properties with neighboring particles.

The two theories each have features they will predict and are not in direct competition with each other. Generally, the theories complement each other. In addition to the comparison with Keffer's (1985) results, model fields will be compared with an earlier study of North Atlantic potential vorticity performed by McDowell, *et al.* (1982).

Section II is a brief review of potential vorticity theories, while in Section III, observations of potential vorticity are discussed. In Section IV the data base and potential vorticity algorithm are discussed. The actual

model output is introduced and described in Section V and model results are compared with observed potential vorticity fields. Conclusions follow in Section VI.

II. THEORIES OF POTENTIAL VORTICITY

Theories depend on whether layers within the thermocline are considered "ventilated," (having an outcrop at the surface) or "unventilated" (no surface outcrop). Note that a layer which outcrops may be poorly ventilated. This can happen if the Ekman pumping at the outcrop is weak or if additional dynamics act to isolate the layer from the boundary conditions at the outcrop. This latter point is the assumption that serves to separate the theory of Luyten *et al.* (1983) from the theory of Rhines and Young (1982a). A layer is considered unventilated if the fluid recirculates several times within the layer before having its properties reset at the surface outcrop. Conversely, a well ventilated layer has its properties reset with essentially every circuit around the gyre. This differs from the geochemical definition of ventilation. To avoid implying something about a layer's oxygen saturation, layers are referred to as either directly ventilated or dynamically isolated from surface boundary conditions. The latter may also be referred to as unventilated, indicating a layer that does not outcrop.

Next, the theories of Rhines and Young (1982a) and Luyten *et al.* (1983) are briefly reviewed. For greater

detail, the reader is referred to the original manuscripts. In a weakly driven layer that does not outcrop, the potential vorticity contours are dominated by $f = f_c + \beta y$ and the lines of constant q will run east-west, intersecting meridional boundaries. Only weak flow is possible if the fluid is to preserve its density and potential vorticity (see Rooth *et al.*, 1978). Any meridional transport is confined to the uppermost layer where the forcing is strong enough to change the fluid's potential vorticity and drive fluid particles across lines of constant q. To allow recirculation, the particles must first forget this new value of q and return to the old. This is the role of the western boundary current of traditional linear models where dissipation removes the energy added by the forcing. The net result is that in a weakly driven, linear ocean, circulation is only allowed where forcing or dissipation is strong: in the upper layer. In deeper layers, the q contours are blocked by meridional coastlines and the forcing is not there to drive the flow across them.

The vertical structure of velocity is more complicated, implying ocean circulation is either nonlinear and strongly driven or, perhaps, diffusive. Modification of the q contours by the flow itself can allow the interior fluid to move meridionally. In the theory of Rhines and Young (1982), the contours of q close on themselves if the

forcing is strong enough, forming rings coinciding with the streamlines. As a result, fluid circulates freely around the gyre while preserving its potential vorticity. This allows the western boundary current to be inertial vice dissipative.

In a following paper, Rhines and Young (1982b) applied an extension of the Prandtl-Batchelor theorem suggesting q should be well-mixed within these closed rings. For this to occur, there must be no sources or sinks of q within the closed contours, the density layer must be dynamically isolated or have a large recirculation index. The recirculation index is a measure of how many times a particle circulates around the gyre before having its potential vorticity or density reset. Therefore, q homogenization is only likely to happen where the density surfaces are deep enough to be isolated from surface forcing, but not so deep as to avoid the influence of the indirect eddy forcing (the $u'q'$ terms) allowing the fluid to spin up and close contours.

An alternative theory of the structure of the thermocline, valid for small recirculation indices, was developed by Luyten *et al.* (1983). In this theory, the thermocline is regarded as ventilated. That is, fluid properties are pumped down from an outcrop along (q, σ_θ) contours via Ekman pumping, deep into the interior of the subtropical gyre, while preserving density and vorticity.

The value of q on a density surface is then its surface value. Knowing q at the surface, or the surface density and an Ekman pumping rate, will completely specify the interior values of q throughout the subtropical gyre, where the q contours can be traced back to the surface. In such a ventilated flow, fluid particles do not tend to recirculate before having their potential vorticity reset (they have a small recirculation index) but are instead pumped directly into the thermocline.

III. OBSERVATIONS OF POTENTIAL VORTICITY

Over the past two decades, several papers have used potential vorticity to discuss circulation patterns and flow paths. Behringer (1972) was likely the first to draw charts of q on isopycnal surfaces. Two charts of the South Atlantic were drawn (Figures 1 and 2). The shallower surface, σ_θ = 30.75 (referenced to 750 db), showed a broad homogenized region of q in the center of the subtropical gyre. The deeper surface, σ_θ = 32.1 (1000 db reference), also showed homogenization, but the charts hint at the intrusion of high q waters from the Indian Ocean. Behringer (1972) used a limited data set. With the more data rich Levitus (1982) climatological data used by Keffer (1985), these features survive but take on a new light, as will be discussed in Section V.

Coats (1981) determined absolute flow vectors in the North Pacific (35° N, 155° W) using a variation of the "β-spiral" method, minimizing the geostrophic noise. He found that in the 400-1300 m range, there were no gradients of potential vorticity on density surfaces in this area. Coats (1983) found large regions of uniform potential vorticity in the South Pacific in the shallow subtropical gyre.

McCartney (1982) used the conservative property of q to trace subpolar "mode" deep water into the subtropical

gyres of the world ocean. Mode water is characterized by a "pycnostad": a thick density layer usually formed by deep wintertime convection. This layer represents a source of low potential vorticity, which can be traced along density surfaces. Two such sources of low q influence the North Atlantic subtropical gyre. One is the well-known 18° water (Worthington, 1959), formed in the intense recirculation regions of the Gulf Stream. The other is formed in the subpolar gyre and enters the subtropical gyre by passing under the North Atlantic Current on deeper density surfaces (McCartney, 1982; McCartney and Talley, 1982). Both are described in further detail in Section V.

McDowell *et al.* (1982) drew maps of the potential vorticity field of the North Atlantic in several different density layers and interpreted them as flow paths. As density increased, the transition from ventilated to dynamically isolated was characterized by vast regions of nearly uniform potential vorticity (Figure 3), in agreement with the theory of Rhines and Young (1982b). At still deeper layers, the circulation had weakened enough that ventilation could again take hold and the layers showed q contours reaching up into the high latitude outcrop windows, allowing easy north-south movement of fluid particles (Figure 4).

Keffer (1985) analyzed the digitized climatological atlas of Levitus (1982). His work shows the North Atlantic

thermocline to be highly anomalous. The extensive outcropping of its density surfaces equatorward of the zero wind-stress curl line, and the resulting strong downward Ekman pumping, allows the surface boundary conditions to control the interior thermocline structure as suggested by Luyten *et al.* (1982). The other oceans show a greater tendency toward homogenization, even at great depth, suggesting relatively complete dynamical isolation. Only in the shallowest layers, where fluid particles are exposed to direct atmospheric forcing is there a tendency for outcrop properties to propagate into the interior. In these regions, winter-time stratification properties are advected into the interior as tongues of high or low q. These results are described in further detail in Section V.

IV. DATA BASE AND METHODS

The data base is model output from the Semtner and Chervin eddy resolving global circulation model (Semtner and Chervin 1992) averaged over the last five years of the model run. An earlier 20-year spin up (Semtner and Chervin 1988) was extended for 12.5 additional years: the first 2.5 years with continued annual mean forcing and the final 10.0 years with climatological monthly forcing using European Center for Medium-Range Weather Forecasting (ECMWF) winds (Trenberth *et al*, 1989). The 0.5°, 20-level grid model produced remarkably realistic three dimensional flow fields, although high latitude eddy resolution was marginal. Seasonal forcing improved the simulation, most notably in the tropics and high northern latitudes. Mid-latitude gyre circulations, western boundary currents, zonal equatorial flows and the Antarctic Circumpolar Current (ACC) exhibit mean and eddy characteristics similar to those observed. Mean flow eddy intensification of the ACC and separated boundary jets are also present.

The model data base was analyzed using the National Oceanic and Atmospheric Administration (NOAA)/Pacific Marine Engineering Laboratory (PMEL) software tool FERRET. FERRET is an interactive program designed for use with very large, well-ordered data sets, allowing the user to work with

explicitly stored variables, abstract mathematical functions, mathematical transformations, and combinations of disk variables. Potential density (σ) was calculated using a FERRET journal file adapted from the simplified equation of state used in the model and the hydrostatic balance. Potential vorticity was calculated as $q=f*d(\sigma)/(dz*\rho)*10^{13}$, where dz is the vertical distance between two density surfaces differing in density by $d(\sigma)$.

The entire procedure was followed for the four density layers listed in Table 1. These density layers were chosen to match those of Keffer (1985) representing depths within the directly forced (layer A), homogenized (B), and isolated (C and D) regions.

TABLE 1. DENSITY LAYERS USED IN THE POTENTIAL VORTICITY CHARTS.

Layer	Ocean	Figure	Midlayer density (σ_θ)	Density Interval (σ)
A	Atlantic	5	26.40	26.30-26.50
	Pacific	6	26.15	26.05-26.25
	Indian	7	26.40	26.30-26.50
B	Atlantic	14	26.75	26.50-27.00
	Pacific	15	26.50	26.25-26.75
	Indian	16	26.75	26.50-27.00
C	Atlantic	22	27.15	27.00-27.30
	Pacific	23		
	Indian	24		
D	Atlantic	31	27.40	27.30-27.50
	Pacific	32		

V. RESULTS

A. UPPER THERMOCLINE (LAYER A)

The pressure of the central density surface (σ_θ = 26.4 in the Atlantic and Indian Oceans, 26.15 in the Pacific Ocean) of the upper-thermocline layer is shown in Figures 5-7. Of note are the steep slopes at approximately 40° S across the South Atlantic and Indian Oceans. These near-vertical slopes are primarily due to convective adjustment in the model. There is some indication from observations that convective overturning produces similar gradients in these areas. However, observations remain too sparse to reach definitive conclusions. Also of interest are the shallow equatorward shelves, or plateaus, of density in the eastern North Atlantic and southern Indian Oceans. These are indicative of tongues of cold water extending toward the equator. In the Atlantic and Pacific Oceans, the model density surfaces follow the observed shape: surfacing at the outcrop regions, reaching their greatest depths near 30° N and S, then shoaling toward the surface at the equator.

Figures 8-10 illustrate the corresponding charts of potential vorticity. Water parcels in this layer pass through the outcrop zone with nearly every circuit, having their properties strongly influenced before they are subducted back into the interior. This "ventilation" of the

thermocline is well illustrated in the Pacific Ocean by loops of relatively high potential vorticity anchored in the outcrop region (Figure 9). In the Atlantic Ocean (Figure 8), the presence of Worthington's (1959) convectively produced "18° water" is not as well defined in the model output as in Keffer's (1985) analysis of Levitus' (1982) data (Figure 11).

The relative maximum in potential vorticity in the vicinity of the Gulf Stream matches well with observations and the homogenized pool south of this area loosely corresponds with the q minimum described by Keffer (1985). This q minimum is also evident in the earlier, hand contoured chart of McDowell *et al* (1982) (Figure 3). Figures 8 and 11 display an equatorward decrease in modelled potential vorticity vice the poleward decrease in q, north of the North Equatorial Current, shown in Figure 3. This can be attributed to the limited data set available to McDowell *et al* (1982). The absence of sources of low potential vorticity east of this low q region results in the water taking on values reflective of the thermocline. These values are then subducted and advected southward (note the q = 10 contour, Figure 8). The homogenized nature of the South Atlantic may be due to the 300 m average depth of the density surface, minimizing the influence of surface conditions. The homogenization of the south central Indian Ocean (Figure 10) can be attributed to this also, with the

average depth of the σ_θ = 26.4 surface at 350 m.

The model Pacific Ocean (Figure 9) and the observed Pacific Ocean (Figure 12) both illustrate a dynamic and well mixed circulation. Of note in the western North Pacific (Figure 9) are the eddy-like features associated with the Kuroshio. Their appearance in five-year-averaged data is evidence of the strength and permanence of these features in the model. The northern and southern tongues of high q along the eastern Pacific Ocean are possibly model representation of the dynamics of the California Current and related upwelling.

In evidence also are equatorward gradients of q that develop on the western side of the subtropical gyres. This makes these areas vulnerable to baroclinic instability (Keffer, 1983). As with the observations, the gradients appear to be due to thermohaline processes vice the dynamics of the recirculating water.

Notably absent are the isolated lenses of high potential vorticity in the eastern North and South Atlantic tropical zones. Keffer (1985) attributes these "domes" to vertical diffusion (Figure 11). In the model, vertical mixing is parameterized according to the method of Pacanowski and Philander (1981), a Richardson number dependent method for tropical oceans. This parameterization may induce smoothing of features smaller than the Richardson number.

The model Indian Ocean (Figure 10) characteristics are similar to those of the observed Indian Ocean (Figure 13). A feature that may be better resolved by the model is the high q region west of Australia. It has been theorized that Leeuwin Current water, upon contact with the ACC, either mixes with the ACC and continues eastward around South Australia or is somehow reflected back into the Indian Ocean. Although observed q (Figure 13) does not resolve this issue, the flow paths indicated in the model output would support the latter. This suggests the need for more detailed observations in this area.

B. UPPER MIDTHERMOCLINE (LAYER B)

The pressure of the central density surface (σ_θ = 26.75 in the Atlantic and Indian Oceans, 26.5 in the Pacific Ocean) of the upper-midthermocline layer is shown in Figures 14-16. This layer, theoretically below the deepest penetration of wintertime convection, should have no mid-gyre sources of potential vorticity. Internal processes, such as salt fingering may be the exception. Nearly all of the recirculation is confined to regions equatorward of the outcrops. The recirculating waters are not exposed to direct atmospheric forcing and are susceptible to homogenization. The surface outcrops of this layer have moved poleward. The average maximum depth of this central density surface is 600 m. Also evident in each of the

basins is the characteristic eastward shoaling of the density gradient. Of interest in the eastern North Atlantic is the westward bulge of the σ_θ = 26.75 surface (Figure 14). This feature would normally be attributed to Mediterranean outflow. The eastern boundary of the model Atlantic Ocean is continuous. Therefore, deep thermal and haline restoring must account for the missing Mediterranean outflow in the model. This feature is not seen in the Keffer (1985) analysis of the Levitus (1982) data (Figure 17). This area is shown as a maximum in thermal and haline deep restoration in the Semtner and Chervin (1992) plots.

Figures 18-20 illustrate the corresponding charts of potential vorticity. All of the oceans show some degree of homogenization, with the Pacific Ocean displaying the greatest amount. However, the model ocean tends less towards homogenization than that observed in the Levitus (1982) data (Figures 17 and 21). Again evident in the eastern North Atlantic (Figure 18) are the effects of deep thermal and haline restoration working to account for the missing Mediterranean outflow.

The tendency toward q homogenization appears to be typical. However, the mechanisms for homogenization differ between basins. In the North Atlantic, the entire gyre shallower than σ_θ = 27.2 is seasonal. That is, winter surface densities are generally greater than this value. Consequently, the entire subpolar gyre is missing from

Keffer's analysis (Figure 17) and the outcrop window lies at the front between these two gyres. There is considerable downpumping of properties from the outcrop into the gyre interior by Ekman pumping. In the model, as in Keffer's results, it appears that North Atlantic homogenization is the result of an intricate arrangement between the geography of the outcrop window and that of the Ekman pumping field. By contrast the analogous density surface in the North Pacific (Figures 15 and 21) has far less exposure to the atmosphere. The outcrop region is confined to a relatively small region in the northwest and no simple, direct ventilation of this density surface is possible.

Keffer (1985) attributes the large values of q in the subpolar gyre of the North Pacific to a light, fresh layer of water in the top 150 m caused by precipitation exceeding evaporation. The density layer shown in Figure 21, lies at the base of this layer and the $f\delta\rho/\delta z$ values are correspondingly high. This precipitation and subsequent vertical mixing acts as a strong source of potential vorticity to the northern gyre and, consequently, q is not homogenized. The corresponding model results, Figure 19, show higher values of q in the North Pacific, yet not as large as those calculated from observations. The difference may be attributable to seasonal and monthly forcing of temperature and salinity values in the model. The Levitus (1982) fields were spline interpolated to daily values for

updating of forcing every three days in the running model. This may have introduced additional smoothing and error.

The high values of q in the northern gyre are not efficiently communicated to the subtropical gyre lying to the south: fluid particles have their potential vorticity reset before they can make an excursion to the adjacent gyre.

Potential vorticity in the South Pacific subtropical gyre appears more homogenized in the model (Figure 19) than in observations (Figure 21). From these figures it can be seen that the area of the winter outcrop of this layer is more extensive in the South Pacific than in the North Pacific. Figure 19 displays the possible outcome of a competition between direct ventilation and a tendency towards homogenization in recirculating gyres. Within the model South Pacific, the homogenization is complete. In the model North Pacific only at the deepest levels, where the outcrops no longer surface, is there a tendency towards homogenization.

C. MIDTHERMOCLINE (LAYER C)

The pressure of the central density surface (σ_θ = 27.15 in the Atlantic, Pacific and Indian Oceans) of the midthermocline layer is shown in Figures 22-24. This layer lies at the base of the wind-driven gyre, in the midthermocline (nominal gyre depth of 800 m). It was

generally chosen to represent the core of various intermediate waters such as the Antarctic Intermediate Water or the lighter variety of Subpolar "Mode" Water described by McCartney (1982). The anomalous feature in the eastern North Atlantic, associated with Mediterranean outflow water, is no longer evident at this depth, approximately 700 m. Figures 25-27 illustrate the corresponding charts of potential vorticity. By this level, the homogenization in the North Atlantic (Figure 25) has disappeared and more certain signs of direct ventilation reappear again. In the observations (Figure 28) the subtropical recirculation of Subpolar Mode Water described by McCartney and Talley (1982) is evident in the uniform small values of q in the northeast corner of the gyre. Once formed in the western part of the European basin, presumably south of the zero wind-stress curl line, this water is then subducted southward between the σ_θ = 27.0 and 27.2 surfaces to appear in the gyre as a relative q minimum. Due to the deep thermal and haline restoration processes in the model eastern North Atlantic, this is not as clearly represented (Figure 25).

The picture in the South Atlantic is strikingly different. At first glance, the gyre appears relatively well mixed compared to the North Atlantic, the range of q values spanning perhaps three-quarters of the total equator-to-outcrop range. But a closer examination of observations

shows lower q water along 40° S lying poleward of slightly higher q water along 30° S - the opposite of the usual β-controlled arrangement. The two waters can be traced back to separate source regions. The lower q water appears to be McCartney's (1977) "Sub-Antarctic Mode Water" with origins in the south-eastern Pacific (see Figure 29), while the higher q water appears to originate from the Agulhas region (see Figure 28) and can be finally traced back to the Indian Ocean (see Figure 30). Keffer's (1985) analysis tends to support McCartney's (1977) conclusions on the origins of Antarctic Intermediate Water (AAIW). Both studies rely on essentially the same technique: tracing low q water from the South Pacific to the South Atlantic.

The picture of this density layer in the model South Atlantic is not as clear. The two separate water types may be inferred from the shape of the 9.0 q contour (Figure 25). Accepting this, it does appear that potential vorticity properties are being injected or diffused from adjacent oceans, rather than a surface outcrop, as in the North Atlantic. Note that in the South Atlantic this surface outcrops at or slightly south of the zero line of wind-stress curl (Baker, 1982), making direct ventilation by downward Ekman pumping difficult. However, the location of the zero wind-stress curl line is questionable as Southern Hemisphere wind field data are relatively unreliable.

As we have seen, this layer is well ventilated in the

North Atlantic and only "indirectly" ventilated in the South Atlantic. However, in the North Pacific (Figure 26) isolation is complete and the layer does not outcrop at all. Despite its somewhat greater depth than the North Atlantic, not only are the North Pacific gyres homogenized, but q is homogenized between gyres as well. Both subtropical and subpolar gyres equilibrate to a small range of q (see the 9.0 contour), extending from 25° to 55° N latitude, and across the full 10,000 km expanse of the North Pacific. The subtropical circulation cannot be driven by the "direct ventilation" mechanism. Instead, momentum is transported downward via eddy stresses (Rhines and Holland, 1979) where it acts to spin up the gyre. Hence, the gyre is indirectly driven by the wind.

Unlike the σ_θ = 26.5-26.7 layer above, at this level the South Pacific is nearly homogenized, being filled with q = 6 contours except for the intrusion of q = 7 water in the southeast. The slight tendency toward nonhomogeneity shows itself as q contours that slope from east-southeast to northeast. Note the low q values in the southeast corner - this is the source of the low q water seen in the South Atlantic in Figure 25.

The Indian Ocean (Figure 27) resembles the South Pacific in that the q field is largely homogenized in the South with a slight tendency towards northwest to southeast ramping (note the q = 9 contour). The small zonal pockets

of low q water centered on 43° S (Figure 30) are attributed to an artifact of the data base in Keffer's (1985) analysis. These are not evident in the model results.

D. LOWER MIDTHERMOCLINE (LAYER D)

The pressure of the central density surface (σ_θ = 27.4 in each of the basins) of the lower-midthermocline layer is shown in Figures 31-33. In the North Pacific (Figure 32), there is no northern surface outcrop of this layer. The density surface itself is relatively flat, with an average depth of 1000 meters. The Indian Ocean (Figure 33) has its southern outcrop along 50° S, the northern boundary of the ACC. The surface's maximum depth is 1400 m in the southwest. The surface outcrop in the North Atlantic (Figure 31) has shrunk and moved northward. The average depth of this relatively flat density surface is 900 m.

Figures 34-36 illustrate the corresponding charts of potential vorticity. Figure 34 shows the q field of the Atlantic ocean in the σ_θ = 27.3-27.5 layer. This layer was chosen because it generally outcrops poleward of the zero wind-stress curl line and hence will be exposed to Ekman suction (rather than Ekman pumping) within the outcrop zone. A still deeper layer might illustrate this better, but may add the additional complication of topographic blocking of contours by the Mid-Atlantic Ridge. This layer acts as the "source" waters for Worthington's (1970) description of the

Norwegian Sea as a "mediterranean basin". Warm, light surface water flows into the Sea at this density, perhaps aided by Ekman suction, and, through atmospheric and oceanographic processes is converted into colder, denser (and slightly fresher) water to be returned at depth.

Even at this great depth (over 1000 m) the North Pacific q field (Figure 35) is still very homogenous. This agrees well with observations (Figure 38). Eddy mixing is probably no stronger in the North Pacific than in the North Atlantic and may even be weaker due to the much larger regions farther from the boundary current. The homogenization process is complete due to the high degree of recirculation within this layer.

Unlike the North Pacific, this density layer outcrops within the South Atlantic, South Pacific, and Indian Oceans (Figures 34-36). Nevertheless, the q field is still very nearly homogenous (although the South Atlantic still shows signs of influence from adjacent oceans). Despite the outcropping, the density layer may be effectively isolated from ventilation anyway, either because of the relatively weak Ekman suction within the outcrops or because the Antarctic Circumpolar Current acts as an effective barrier to ventilation by winding q contours around the Antarctic continent. The flow path from the eastern North Atlantic to deep within the subtropical gyre can be seen in each of the Atlantic q charts (Figures 4, 34 and 37). The broad

homogenized region in the southern Indian Ocean (Figure 36) corresponds well with observations (Figure 39). The east-west q contours in the central Atlantic and Pacific Oceans and the northern Indian Ocean, seen in Layer C and again in Layer D, are characteristic of weakly driven layers that do not outcrop. The potential vorticity contours are dominated by $f = f_0 + \beta y$, indicating a weakly driven flow, with the earth's vorticity dominating the potential vorticity fields.

VI. CONCLUSIONS

Charts of potential vorticity (q) within four different density layers, calculated from a high resolution model that used known bathymetry, observed ship winds, and historical temperature and salinity data to simulate global ocean circulation were compared with potential vorticity calculated from a computerized climatological atlas.

Overall, the representation of global ocean circulation with 0.5° grid size and biharmonic mixing is reasonably good. Nevertheless, improved resolution is needed to model the instabilities of mid-latitude western boundary currents and those of the Antarctic Circumpolar Current. Initial results from an improved 1/6° grid size simulation are promising.

New 1/4° and 1/6° simulations, developed at the Naval Postgraduate School and the Los Alamos National Laboratory in recent months and currently running on the Cray Y-MP/8 at the National Center for Atmospheric Research and the 1024-node CM-5 at Los Alamos, are showing promising results in providing improved resolution of ocean circulation. The 1/6° model now extends up to 78° North and the deep diagnostic forcing terms have largely been removed from both models. The 1/4° resolution model treats the oceanic barotropic mode by the free-surface method of Killworth *et*

al (1991), vice the previous rigid-lid assumption. This reduces computer requirements with grid sizes smaller than 1/2° and allows more realistic geometry with many islands. Additionally, the models use observed wind and thermohaline forcing together with satellite altimetric data. Analysis of model output will show whether these modifications have improved representation of potential vorticity fields.

The density structure of the model is quite similar to observations. It might be argued that the model was started with the observed density structure and should remain near it. However, most of the comparisons made here are in and above the permanent pycnocline, areas being actively modified by surface processes, either directly through convection, or indirectly through ventilation and subduction. After accounting for the weak restoring below 710 m and the parameterization of surface heat and moisture fluxes, the model results can be considered essentially unconstrained. Information in the thermocline range 25-710 m, outside of polar latitudes, has established itself freely over a twenty year simulation (Semtner and Chervin 1992).

As with the density structure, the potential vorticity of the model solution in the density layers above the main pycnocline agrees well in the pattern and values with the estimates made from observations. The expected homogenization occurs below the directly forced layers and a

ventilation path from the northeastern Atlantic is evident.

The deep thermal and haline restoring terms in the eastern North Atlantic, there to account for the missing Mediterranean outflow, produce an unrealistically large signature, when interpreted from the potential density and potential vorticity charts. The removal of the deep diagnostic forcing terms in a more recent model run may solve this problem. Integrating a Mediterranean Sea regional model into the global model might also provide more realistic results, providing the narrow Strait of Gibraltar is treated properly.

The lack of resolution of the Arctic Ocean causes problems which robust diagnostic forcing cannot completely remedy. Understanding the effects of the Arctic Ocean and its marginal seas on the production of North Atlantic Deep Water and the separation of the Gulf Stream, would be improved by adding the Arctic domain to the model. As noted in Semtner and Chervin (1992), the model Gulf Stream separates from the North American continent farther north than observed. This may account for the disparity in potential vorticity contours and values seen in this area. Improved resolution in higher latitudes thus hopefully improving treatment of the Labrador current, may improve the positioning of the model Gulf Stream.

Convection and other high latitude processes seem poorly treated, even with a seasonal cycle of forcing. More

effective treatments of these processes will be required in the future. To examine present-day ocean circulation, diagnostic forcing can be employed to augment convective adjustment and maintain deep and bottom waters of the North Atlantic and the southern ocean. The results of a 1/4° model run with the deep diagnostic forcing terms removed showed improvements in resolving deep and bottom water currents.

In the southern high latitudes, however, the lack of winter hydrographic data and the unreliable wind stress data, especially for a differentiated quantity like wind stress curl, make it difficult to evaluate parameterizations and model performance. It has come to the point of model output exhibiting interesting southern ocean features, not previously observed, whose existence are then confirmed with further observations.

Away from boundaries where relative vorticity is known to be significant, the charts of potential vorticity appear to be good indicators of the dynamics that persist within particular density intervals. The transition from the direct wind-driven circulation within the gyres to the source-sink regime of the main thermocline is observed in each of the basins.

Four separate flow domains are present. In regions of Ekman downwelling the surface density distribution is prescribed. This regions breaks further into a three-fold

subdivision. First, there exists a constantly refreshed, ventilated region in which all fluid layers are in motion. On the periphery of this ventilated region, shadow zones emerge traced by potential vorticity contours emerging from meridional boundaries. These shadow zones may bound regions of uniform potential vorticity or regions which are stagnant. The fourth zone occurs in regions of Ekman upwelling. The surface density field there is no longer arbitrarily prescribed. Instead, density surfaces are pulled, one after another, to the surface in response to Ekman suction.

Although the regions of ventilation and homogenization are spatially distinct, they interact and affect one another non-linearly since the regions must combine to support the Sverdrup transport.

A valuable feature of using potential vorticity on density surfaces to determine flow paths is it allows three dimensional flow analysis. With larger vertical density variations than in the horizontal throughout the majority of the global ocean, vertical resolution is an important factor. At 20 layers, the model provides a fair representation of vertical thermocline structure. Increased vertical resolution may improve that representation

Further improvements in the physics of the simulation and vertical resolution will improve the model's representation of oceanic circulation and potential

vorticity. In all, the model represents general flow characteristics as determined by charts of potential vorticity quite well. Recent model upgrades, as mentioned above, and planned improvements in forcing and parameterizations will continue to improve the model representation of ocean circulation. Successive improvements come closer to resolving disturbances at the local scale of deformation as well as through some portion of an inertial cascade, which is one of the main goals of ocean modeling.

LIST OF REFERENCES

Baker, D. J., 1982: A note on Sverdrup balance in the Southern Ocean. *J. Mar. Res.*, **40**(Suppl.), 21-26.

Behringer, D. W., 1972: Investigations of large scale oceanic circulations using historical hydrographic data. Ph.D. Dissertation, University of California-San Diego. 145 pp.

Boyer, T., and Klinck, J. M., 1992: Potential vorticity and density surfaces in an eddy resolving, North Atlantic simulation (in preparation). *J. Geophys. Res.*, ?

Coats, D. A., 1981: An estimate of absolute geostrophic velocity from the density field in the Northeastern Pacific Ocean. *J. Geophys. Res.*, **86**, 8031-8036.

--------, 1983: The absolute flow field in the South Pacific Ocean. *Deep-Sea Res.*, **30**, 1033-1057.

Keffer, T., 1985: The ventilation of the world's oceans: maps of the potential vorticity field. *J. Phys. Oceanogr.*, **15**, 509-523.

Killworth, P. D., D. J. Webb, D. Stainforth, and S. M. Patterson, 1991: The development of a free-surface Bryan-Cox-Semtner ocean model. *J. Phys. Oceanogr.*, **21**, 1333-1348.

Levitus, S., 1982: *Climatological Atlas of the World Ocean*. NOAA Prof. Paper 13. U.S. Govt. Printing Office, Washington, D.C., 173 pp.

Luyten, J. R., J. Pedlosky and H. Stommel, 1983: The ventilated thermocline. *J. Phys. Oceanogr.*, **13**, 292-309.

McCartney, M. S., 1977: Subantarctic mode water. *A Voyage of Discovery: George Deacon 70th Anniversary Volume*, Suppl., *Deep-Sea Res.*, M. Angel, Ed., 103-119.

--------, 1982: The subtropical recirculation of mode waters. *J. Mar. Res.*, **40**(suppl.), 427-464.

--------, and L. D. Talley, 1982: The subpolar mode water of the North Atlantic Ocean. *J. Phys. Oceanogr.*, **12**, 1169-1188.

McDowell, S., P. Rhines and T. Keffer, 1982: North Atlantic potential vorticity and its relation to the general circulation. *J. Phys. Oceanogr.*, **12**, 1417-1436.

Pacanowski, R. C., and S. G. H. Philander, 1981: Parameterization of vertical mixing in numerical models of tropical oceans. *J. Phys. Oceanogr.*, **11**, 1443-1451.

Pedlosky, J, 1983: Eastern boundary ventilation and the structure of the thermocline. *J. Phys. Oceanogr.*, **13**, 2038-2044.

--------, and W. R. Young, 1983: Ventilation, potential-vorticity homogenization and the structure of the ocean circulation. *J. Phy. Oceanogr.*, **13**, 2020-2037.

Rhines, P. B., and W. R. Holland, 1979: A theoretical discussion of eddy-driven mean flows. *Dyn. Atmos. Oceans*, **3**, 289-325.

--------, and W. R. Young, 1982a: A theory of wind driven ocean circulation, I. Mid-ocean gyres. *J. Mar. Res.*, **40**(suppl.), 559-596.

--------, and --------, 1982b: Homogenization of potential vorticity in planetary gyres. *J. Fluid Mech.*, **122**, 347-368.

Rooth, C., H. Stommel and G. Veronis, 1978: On motion in steady layered geostrophic models. *J. Oceanogr. Soc. Japan*, **34**, 265-267.

Semtner, A. J., and R. M. Chervin, 1988: A simulation of the global ocean circulation with resolved eddies. *J. Geophys. Res.*, **93**, 15502-15522.

--------, and --------, 1992: Ocean general circulation from a global eddy-resolving model. *J. Geophys. Res.*, **97**, 5493-5550.

Trenberth, K. E., J. G. Olson and W. G. Large, 1989: A global ocean wind stress climatology based on ECMWF analyses. NCAR Tech Note NCAR/TN-338+STR, 93 pp.

Worthington, L. V., 1959: The 18° water in the Sargasso Sea. *Deep-Sea Res.*, **5**, 205-211.

--------, 1970: The Norwegian Sea as a mediterranean basin. *Deep-Sea Res.*, **17**, 77-84.

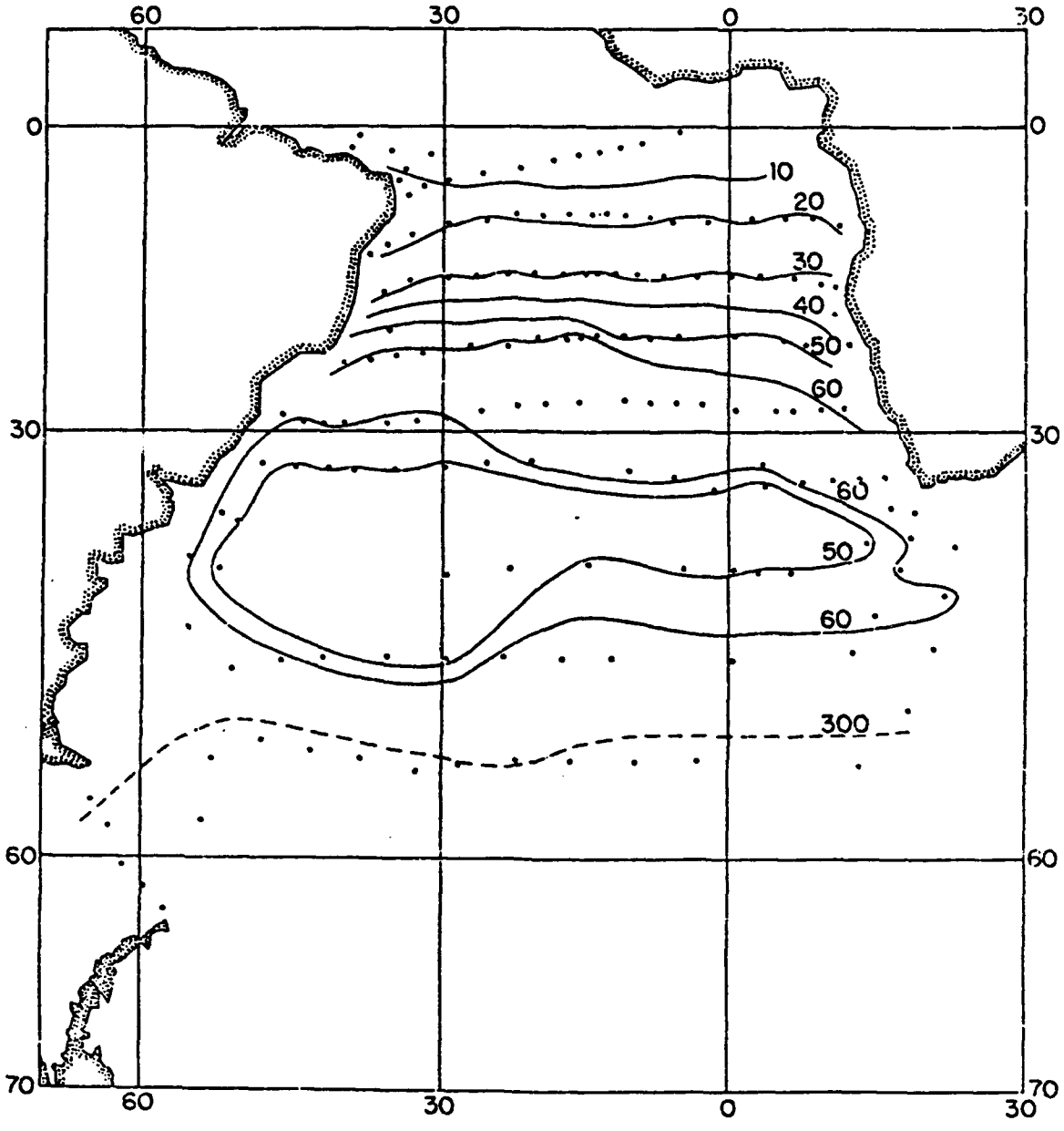

Figure 1. South Atlantic Ocean. Contours of $2\Omega \sin(\delta\sigma_\theta/\delta z)$ (DPV/ρ contours) on the potential density surface σ_θ = 30.75 g_1^{-1}. The potential density surface is referred to a depth of 750 m. A difference of ten units corresponds to a difference of 10^{-8} $g_1^{-1}m^{-1}$ s^{-1} (From Behringer, 1972).

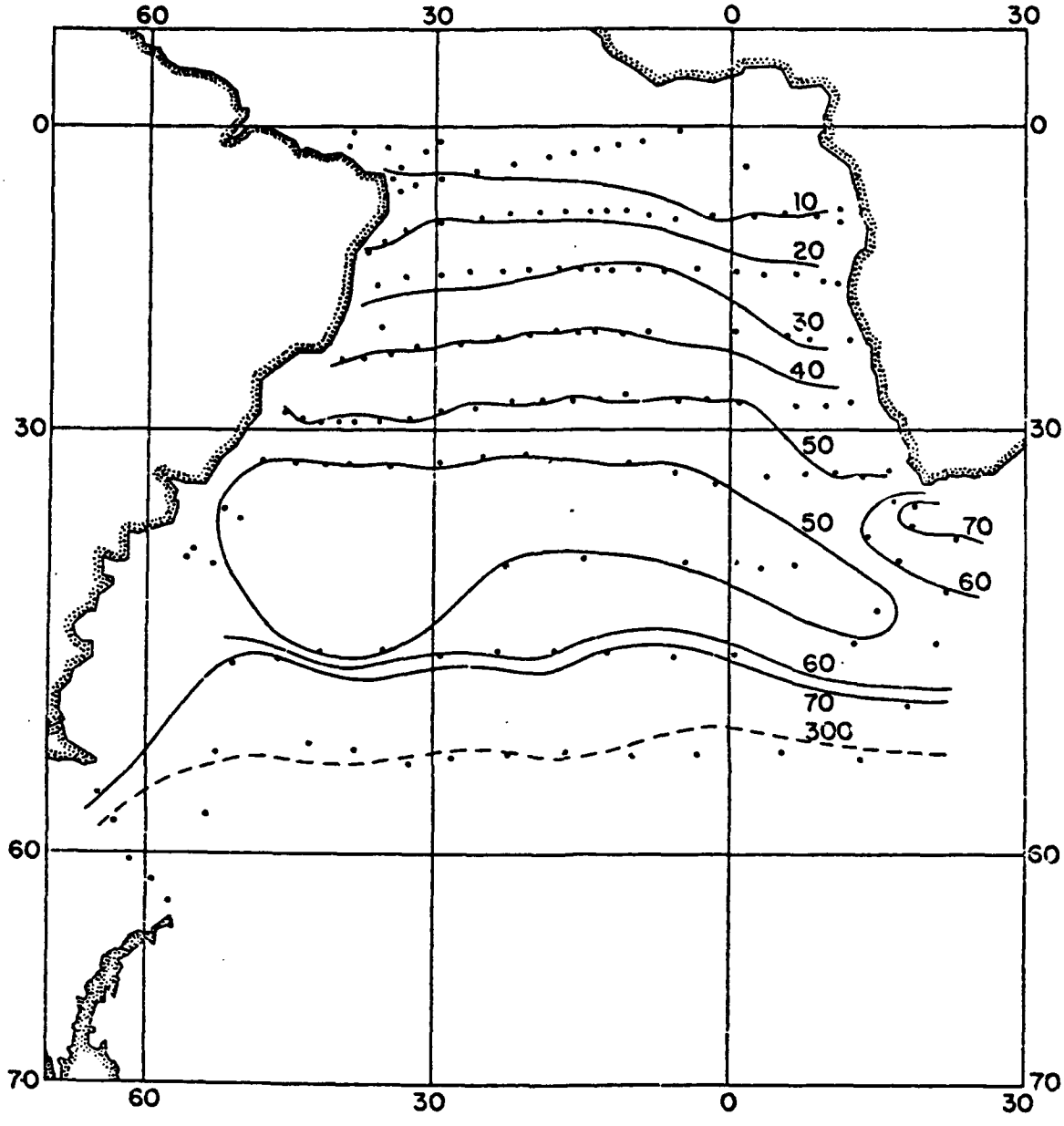

Figure 2. South Atlantic Ocean. Contours of $2\Omega \sin(\delta\sigma_\theta/\delta z)$ (DPV/ρ contours) on the potential density surface σ_θ = 32.10 g_1^{-1}. The potential density surface is referred to a depth of 1000 m. (From Behringer, 1972).

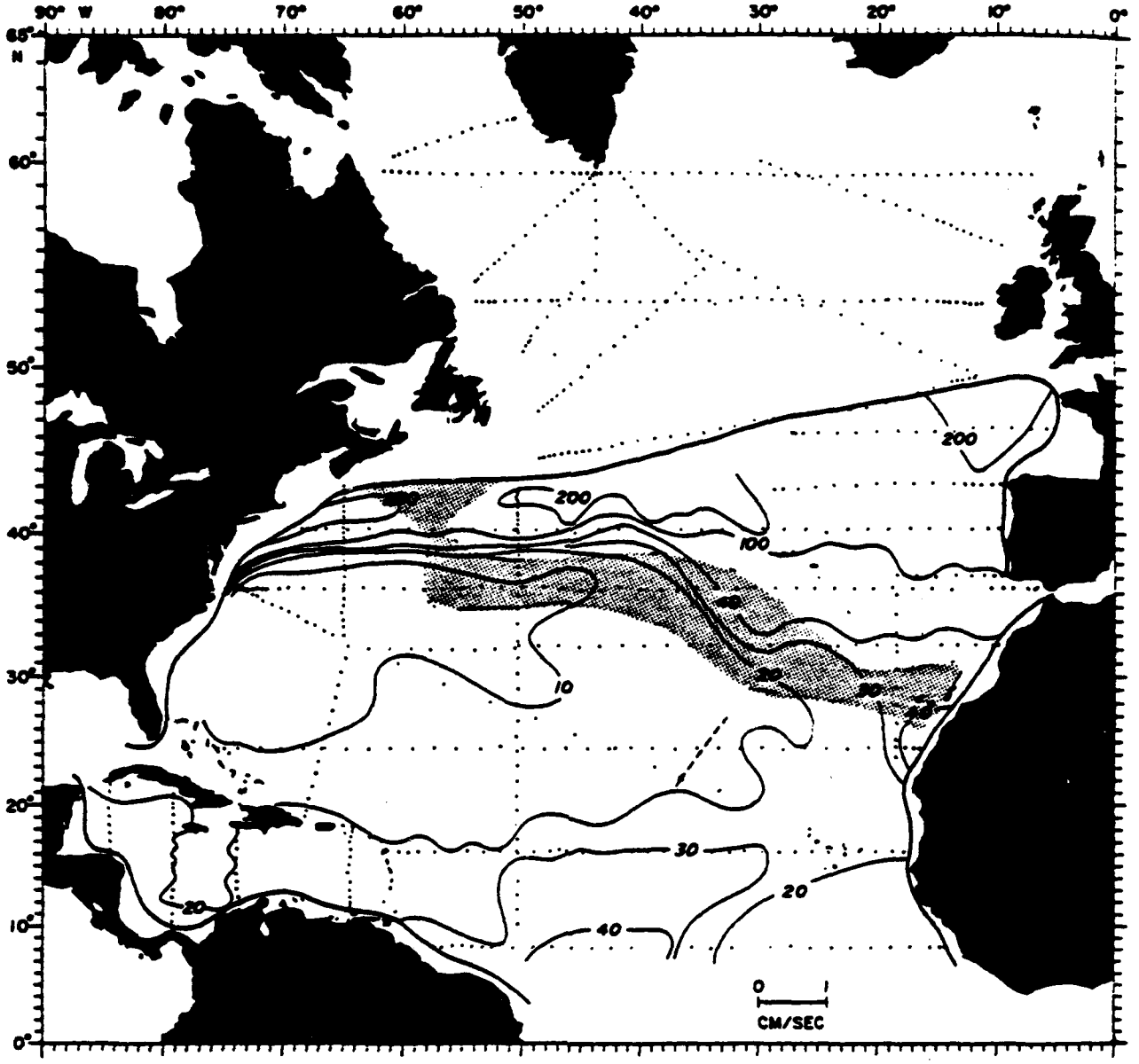

Figure 3. Potential vorticity (10^{-13} $cm^{-1}s^{-1}$) between the σ_θ = 26.3 and 26.5 surfaces. The bold line represents the outcrop of the 26.0 surface during the observation period. The stippled area lies between the winter outcrops of the two surfaces. The nonlinear control of q contours is clearly evident. Fluid can move great distances meridionally, while conserving its potential vorticity. Note the northward decrease in q in the North Equatorial Current region. This marks this area as a likely region of baroclinic instability (From McDowell *et al*, 1982).

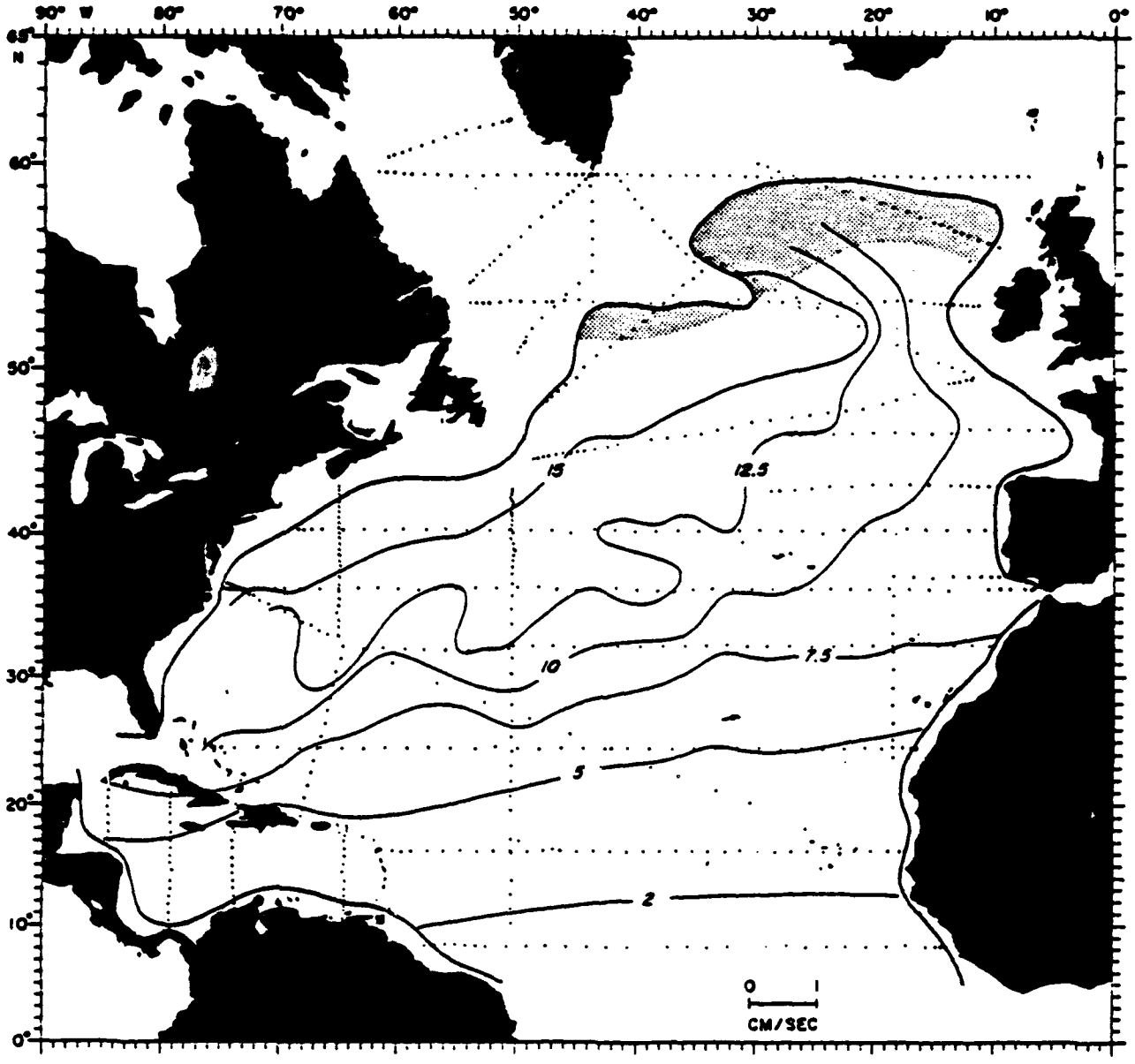

Figure 4. Potential vorticity between the σ_θ = 27.3 and 27.6 surfaces. Other features as in Figure 3. The q contours stretch from northeast to southwest, allowing easy communication of fluid between high latitudes and the deep subtropical Atlantic (From McDowell *et al*, 1982).

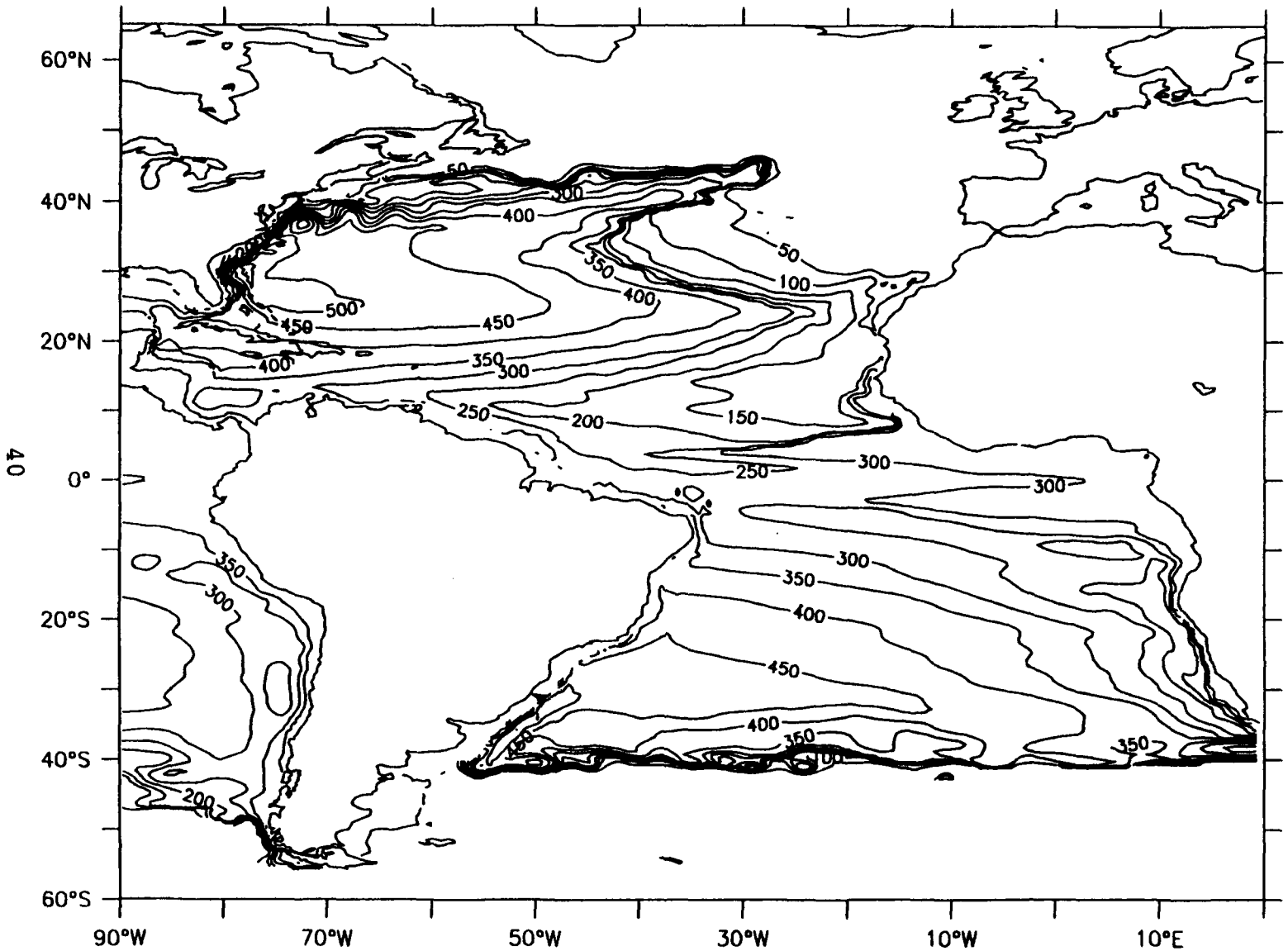

Figure 5. Depth in meters of the σ_θ = 26.4 surface (Layer A), Atlantic Ocean.

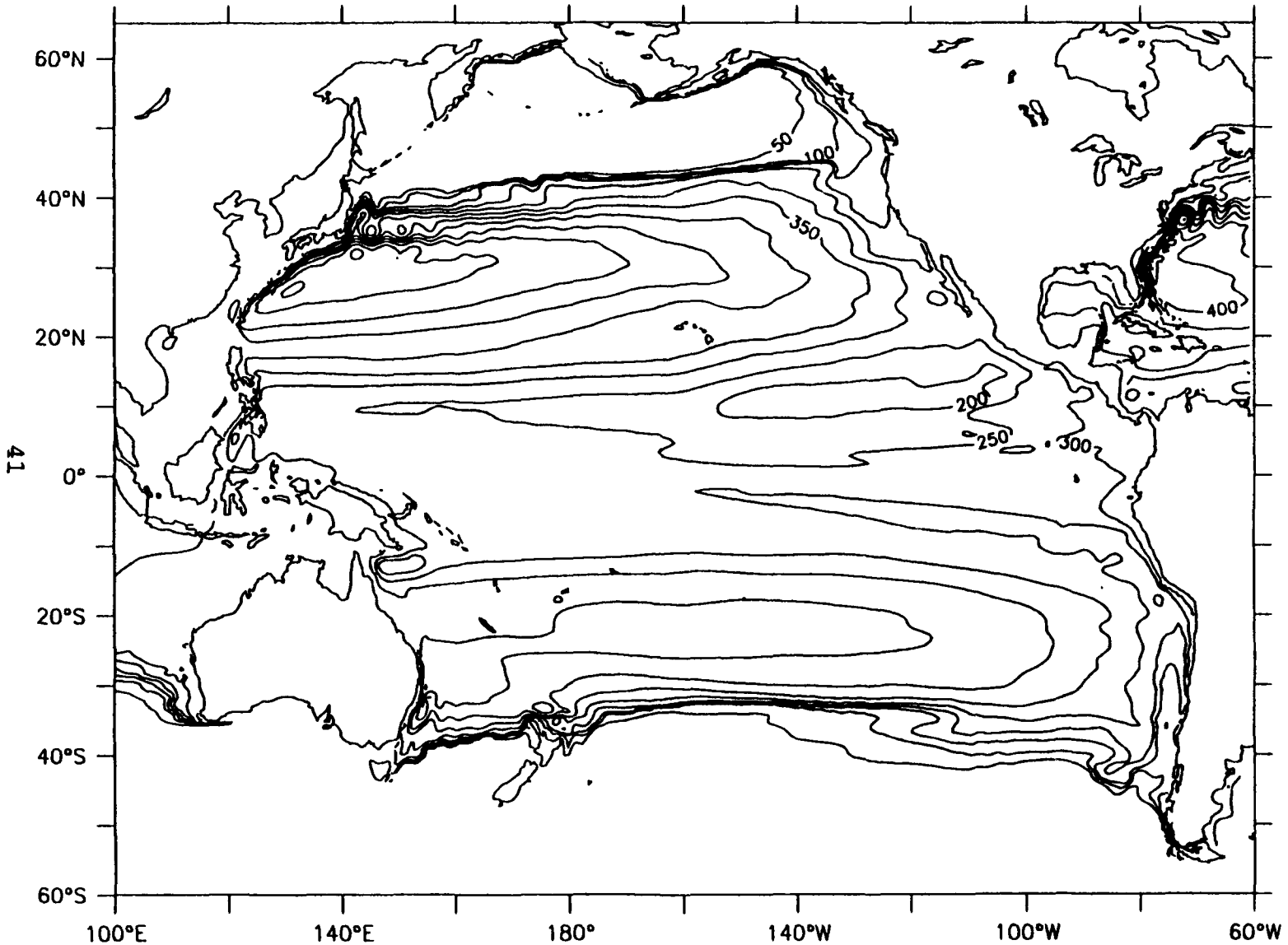

Figure 6. Depth in meters of the σ_θ = 26.15 surface (Layer A), Pacific Ocean.

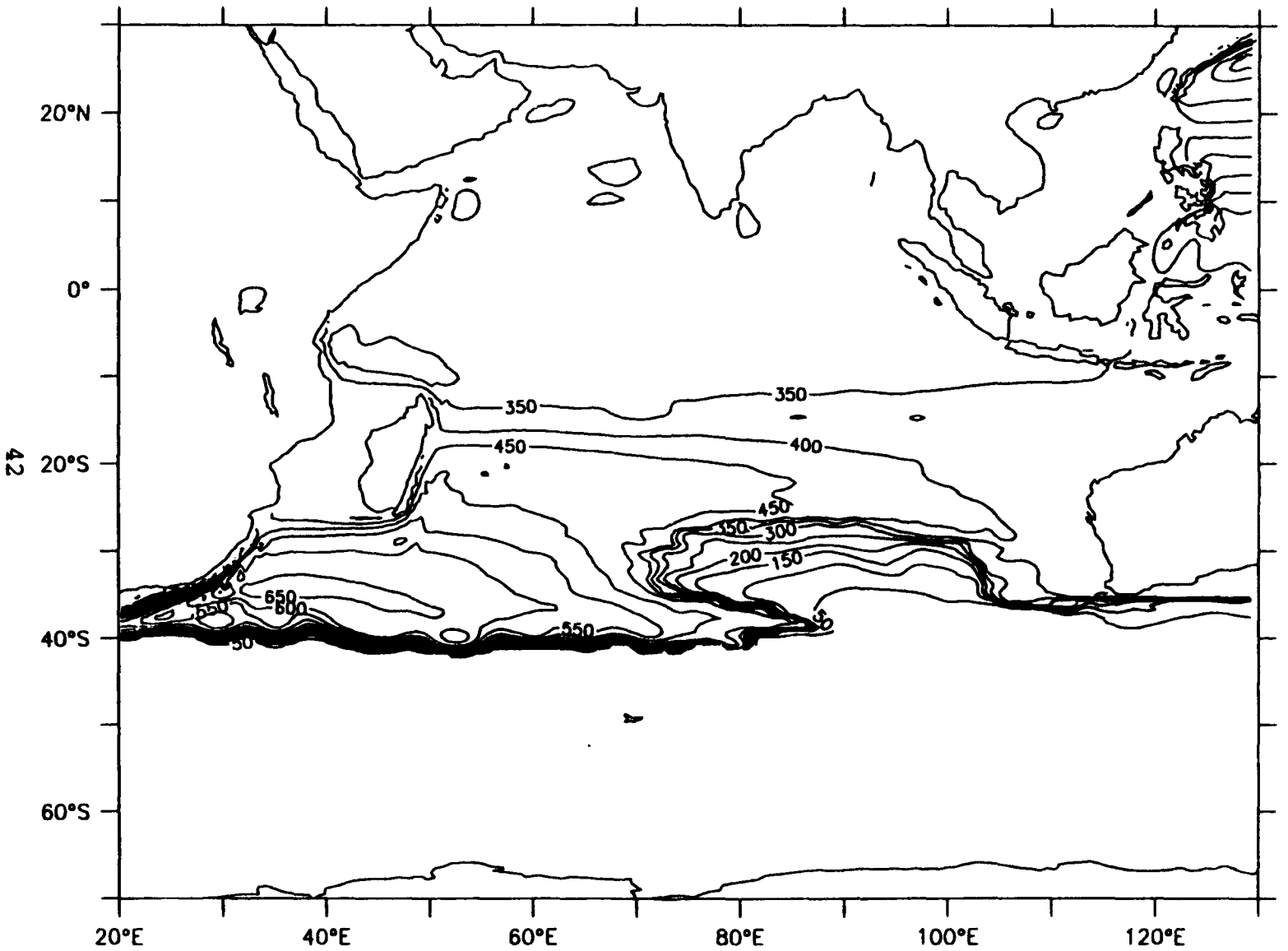

Figure 7. Depth in meters of the σ_θ = 26.4 surface (Layer A), Indian Ocean.

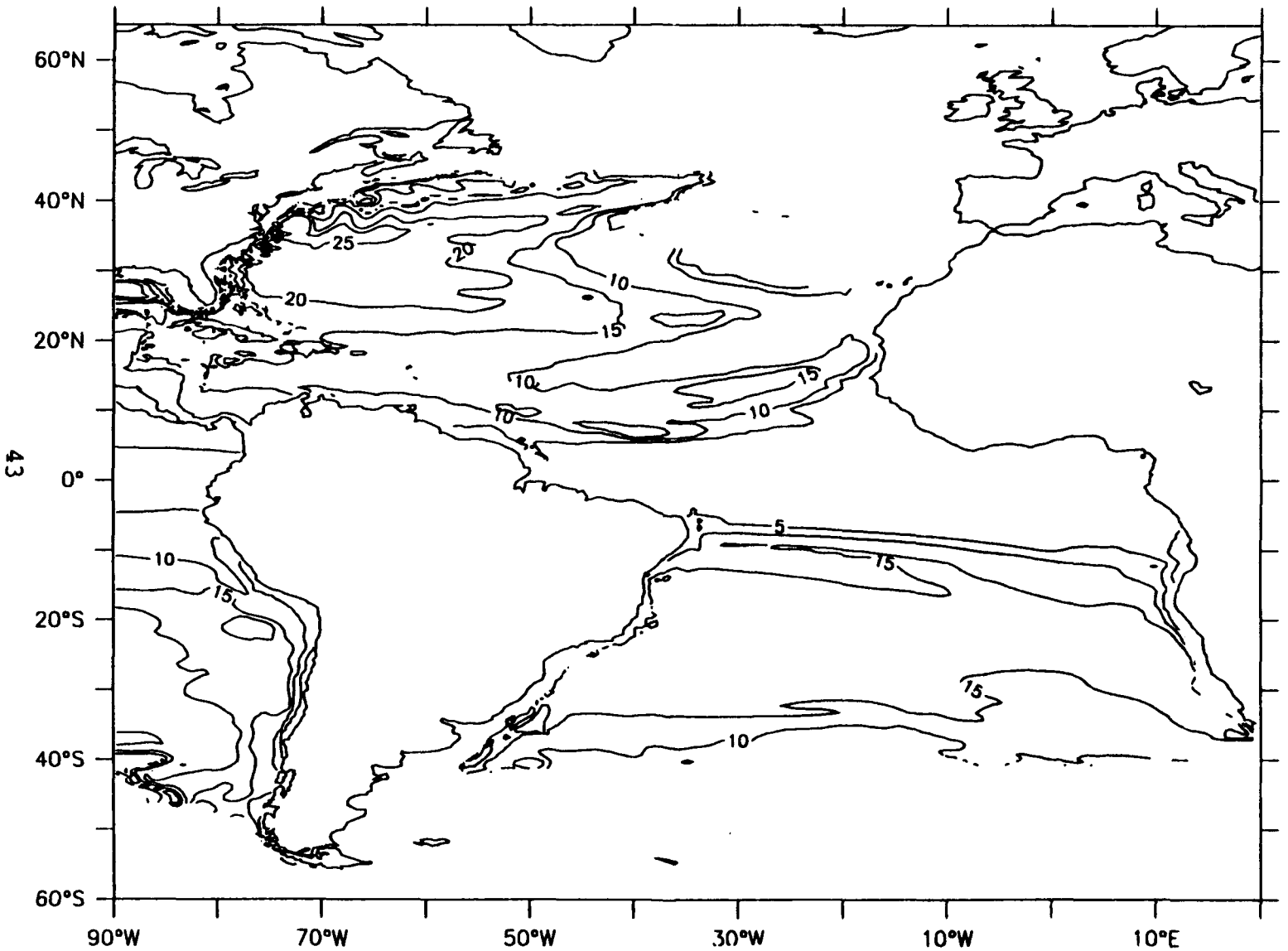

Figure 8. Potential vorticity of the σ_θ = 26.3-26.5 interval (Layer A), Atlantic Ocean.

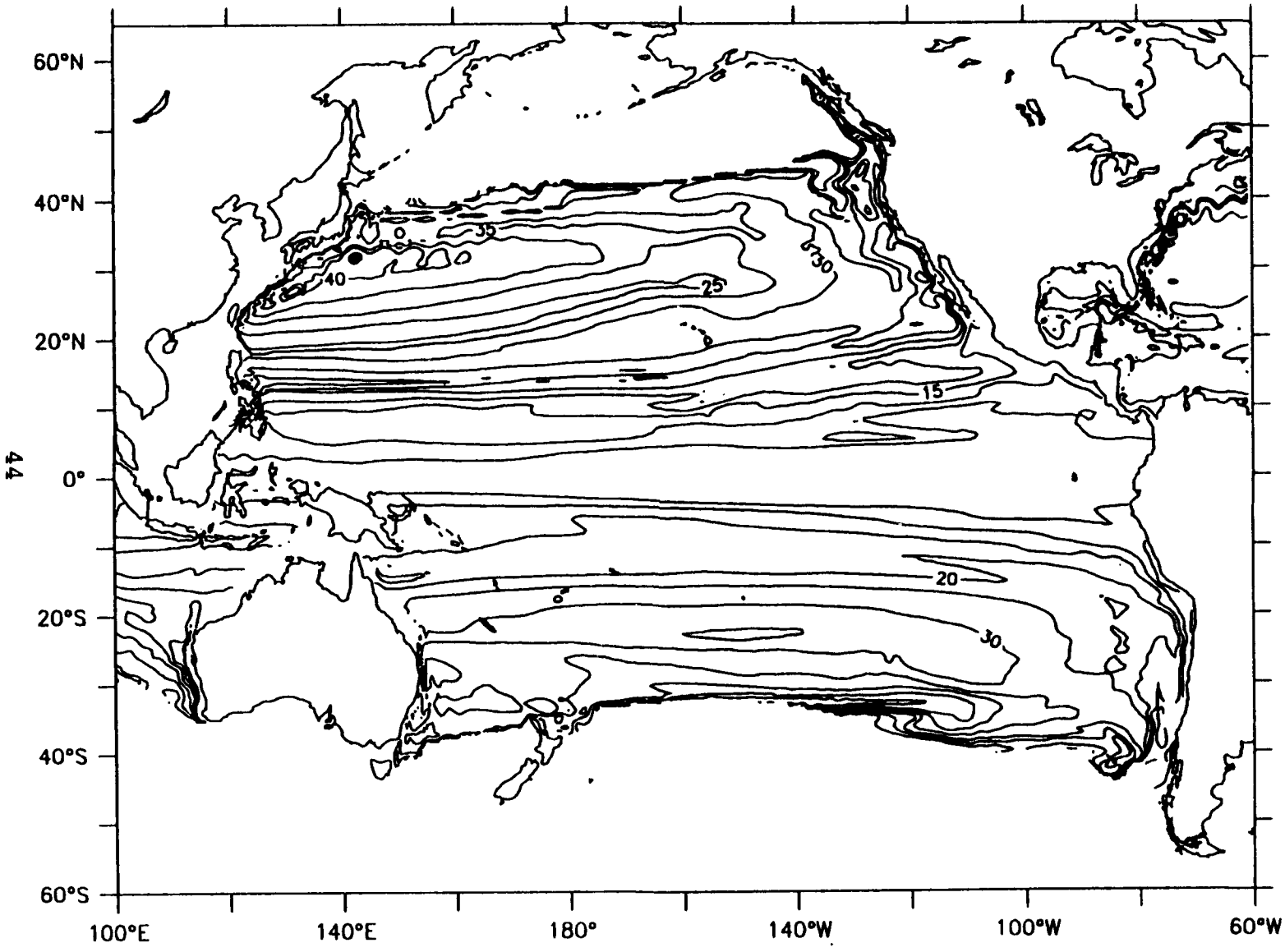

Figure 9. Potential vorticity of the σ_θ = 26.05-26.25 interval (Layer A), Pacific Ocean.

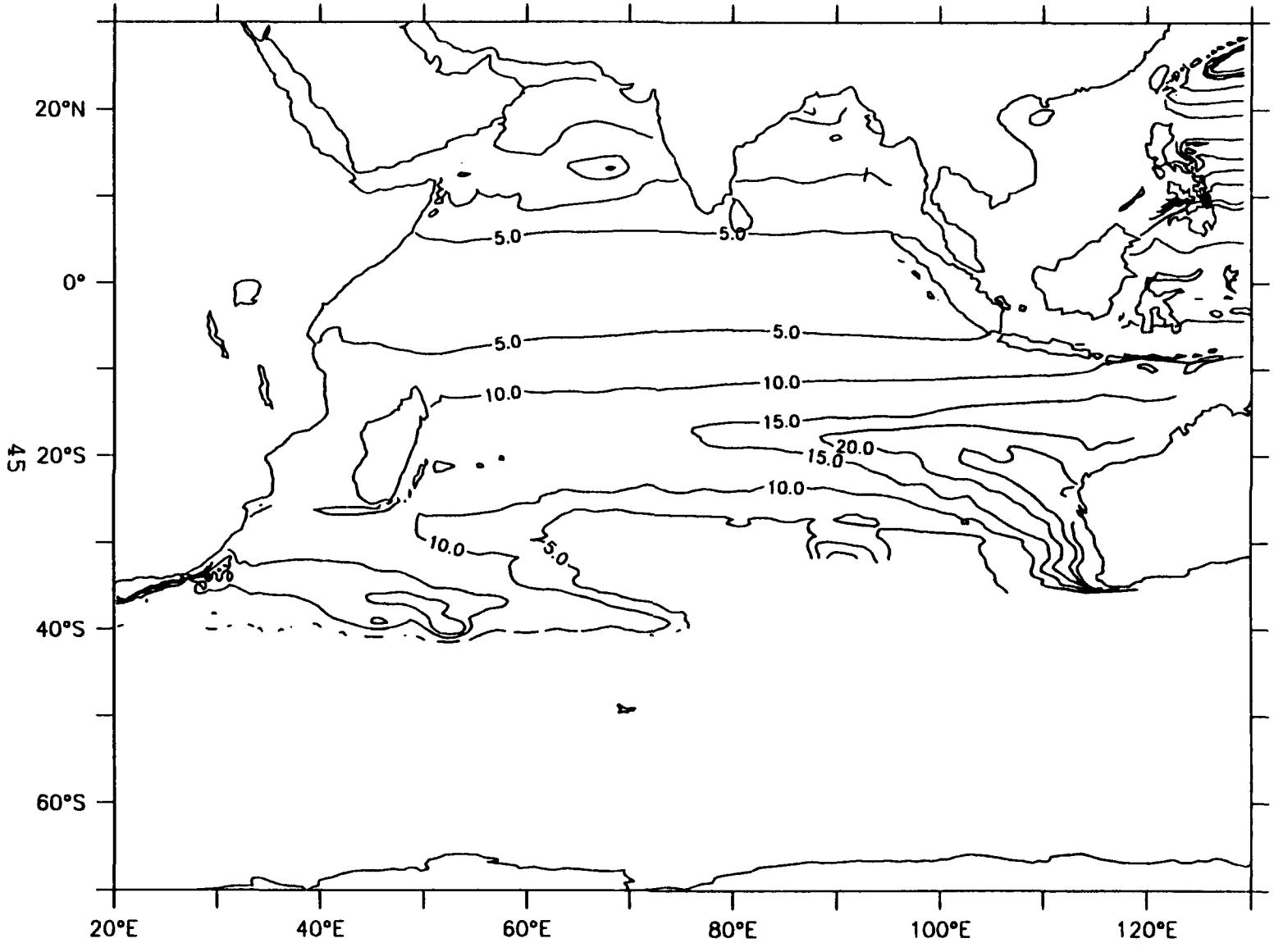

Figure 10. Potential vorticity of the σ_θ = 26.3-26.5 interval (Layer A), Indian Ocean.

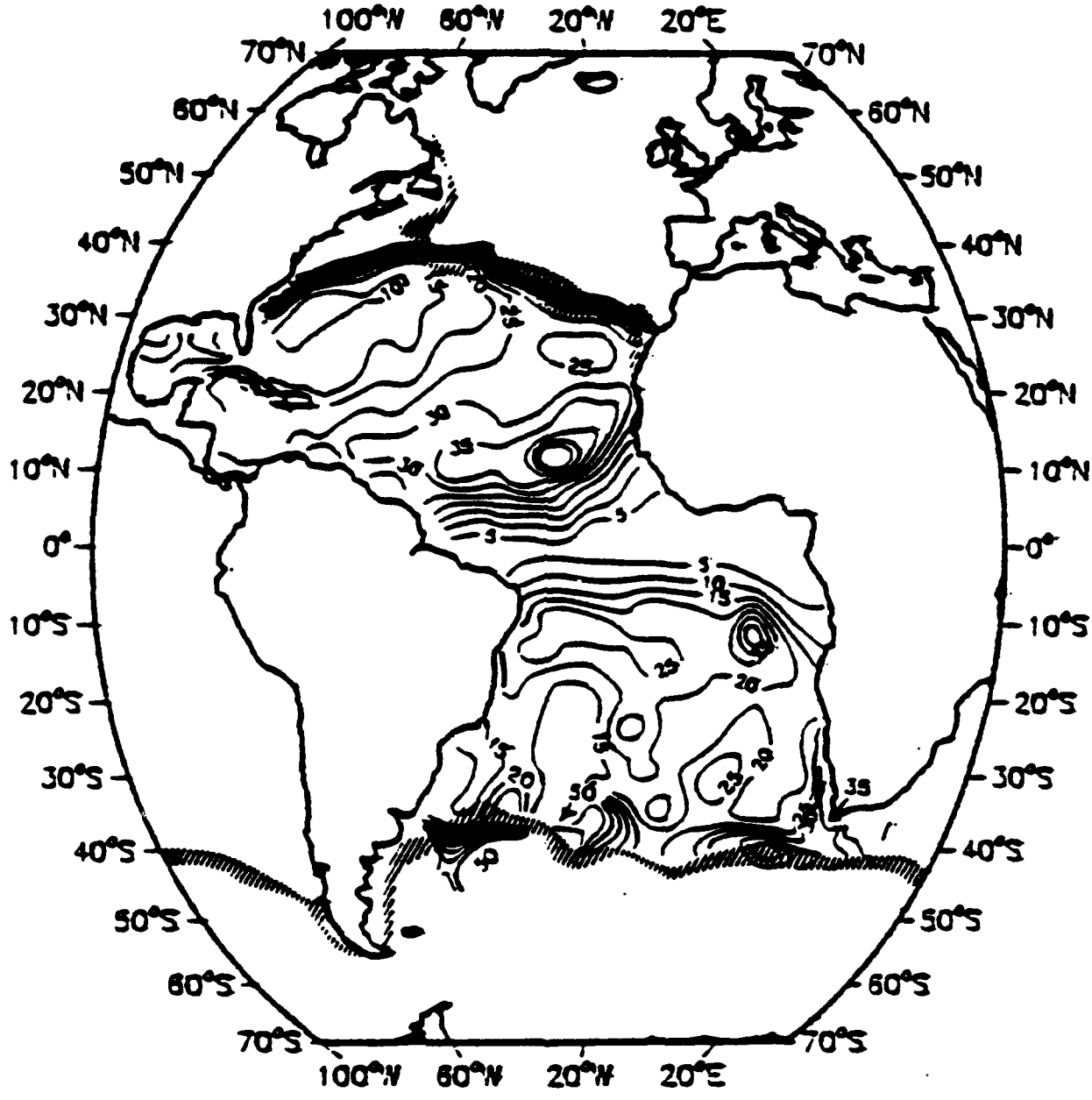

Figure 11. Potential vorticity of the σ_θ = 26.3-26.5 interval (Layer A), Atlantic Ocean (10^{-13} $cm^{-1}s^{-1}$). The striped regions mark the winter outcrop window of this layer. Note the low q region in the Western North Atlantic. This is the 18° Water thermostad of Worthington (1959) (From Keffer, 1985).

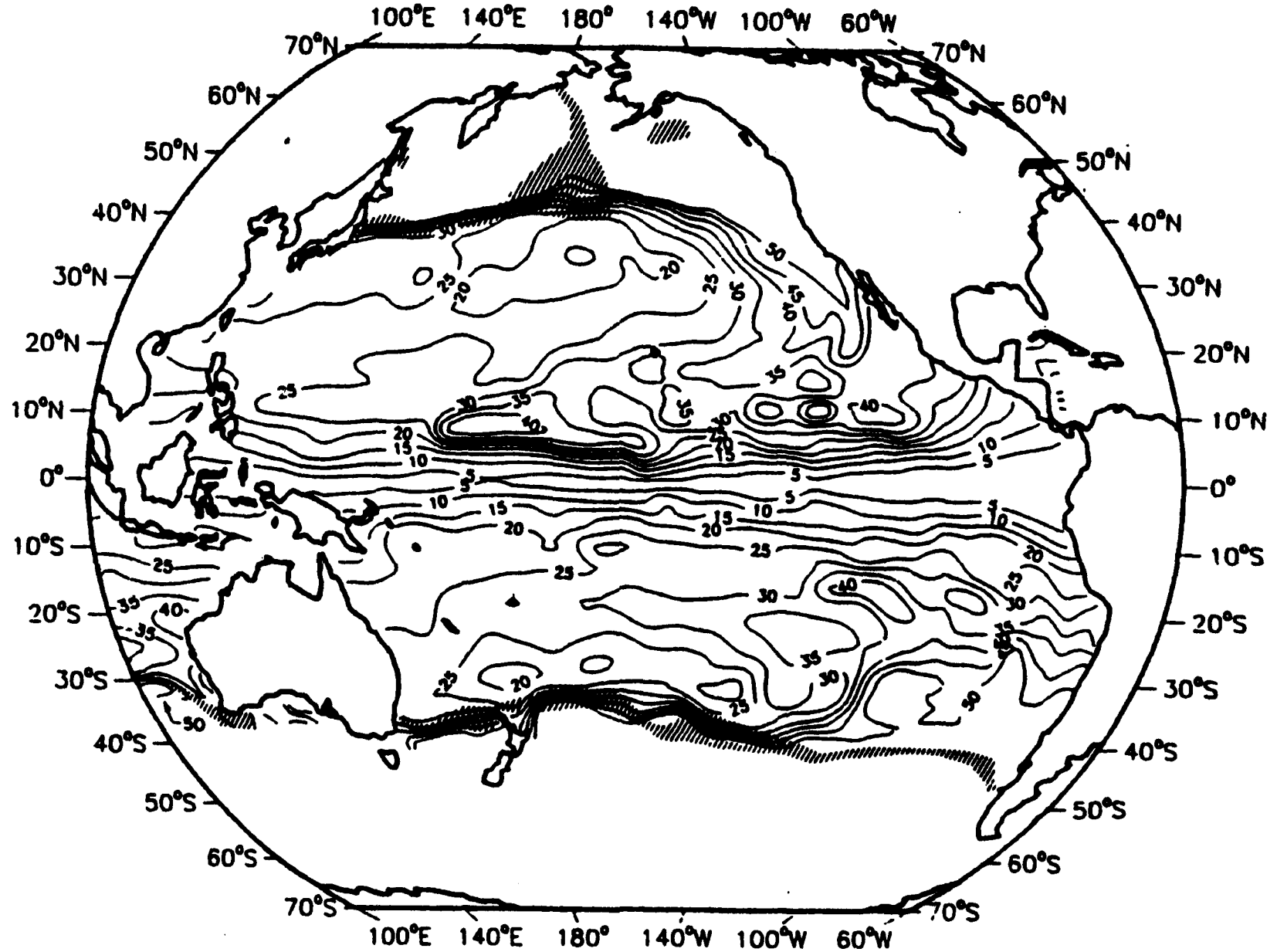

Figure 12. Potential vorticity of the σ_θ = 26.05-26.25 interval (Layer A), Pacific Ocean. Other features as in Figure 11. Note the high q "tongue" entering the eastern sides of the North and South Pacific (From Keffer, 1985).

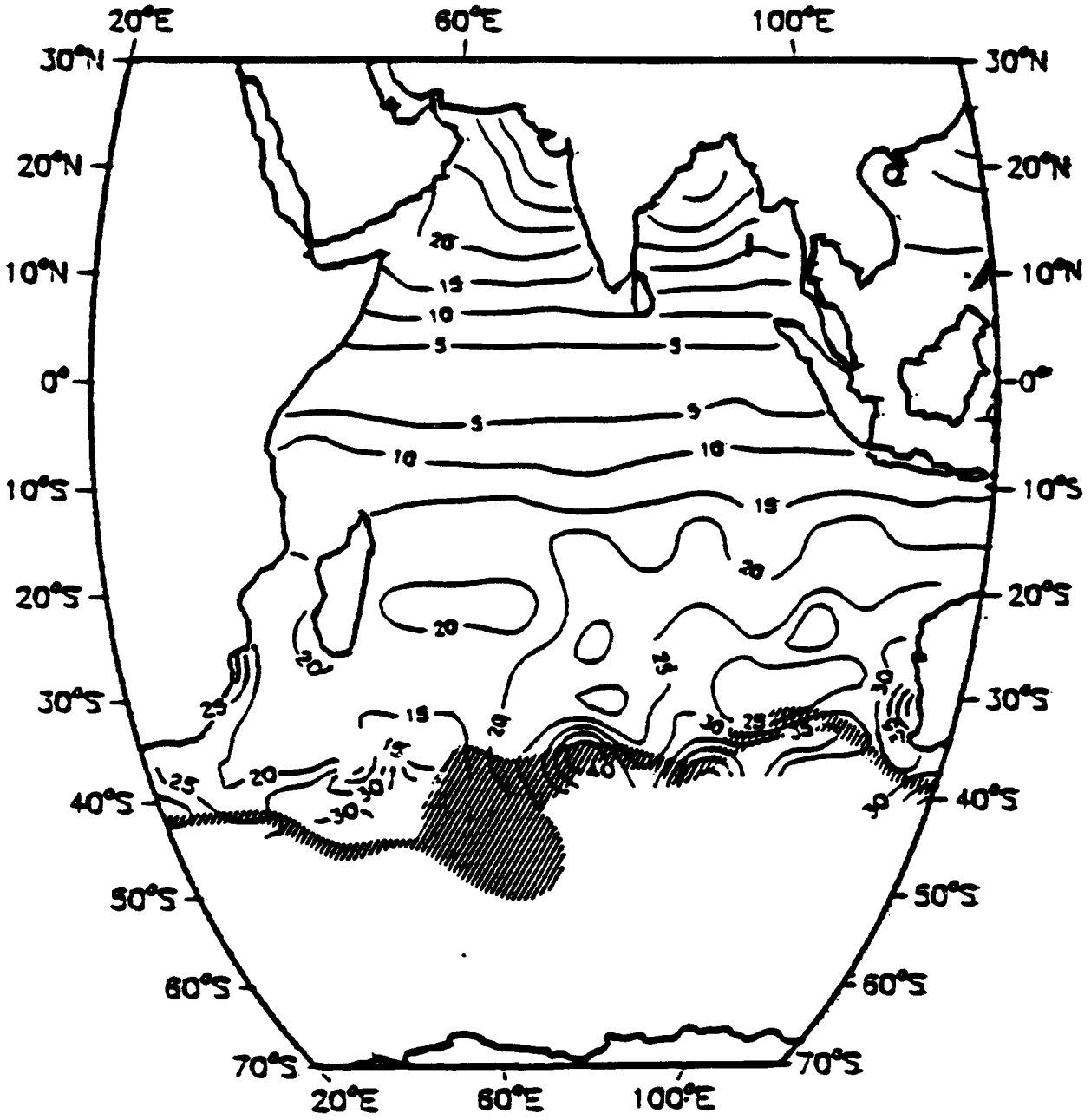

Figure 13. Potential vorticity of the σ_θ = 26.05-26.25 interval (Layer A), Indian Ocean. Other features as in Figure 11 (From Keffer, 1985).

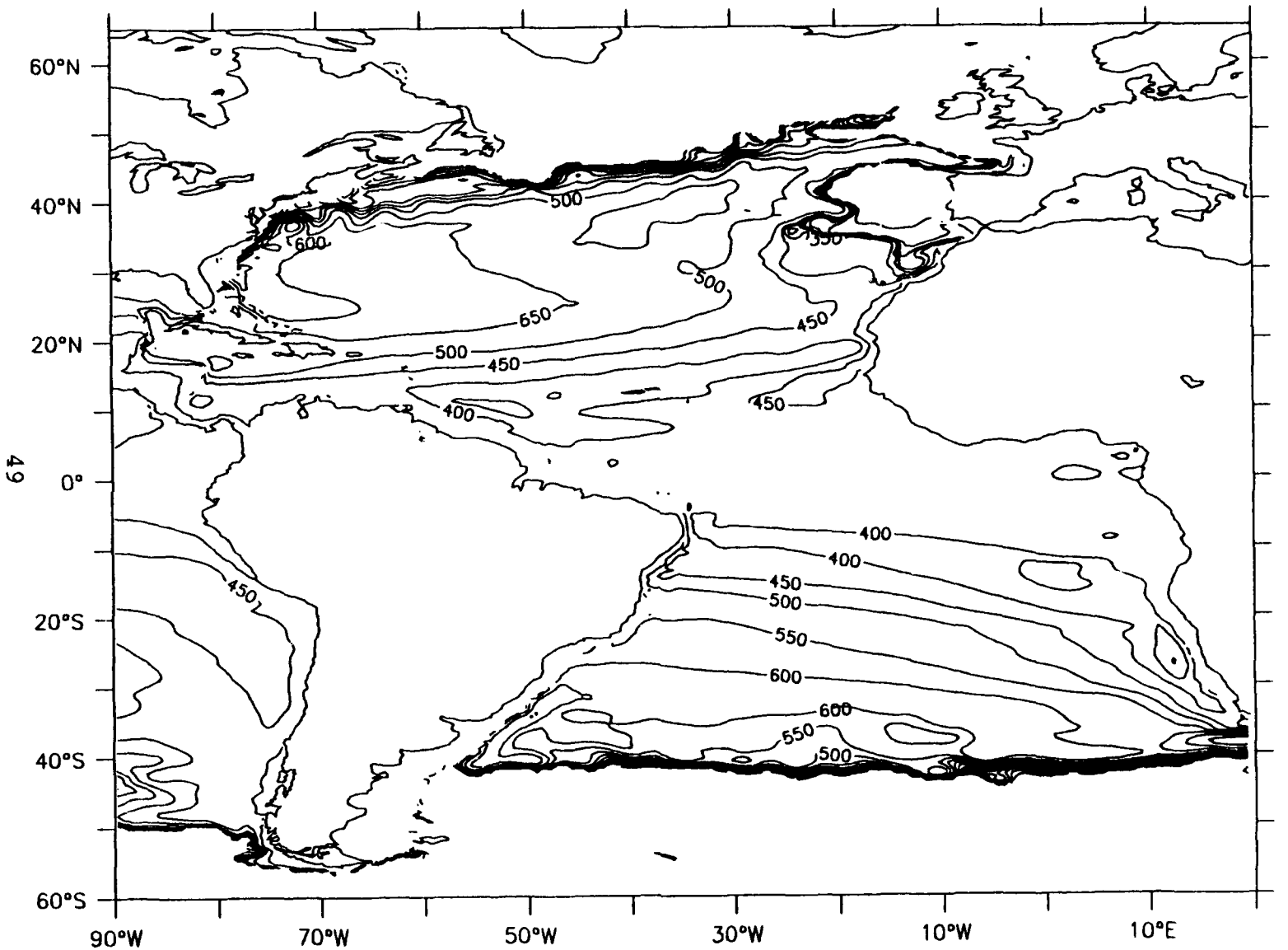

Figure 14. Depth in meters of the σ_θ = 26.75 surface (Layer B), Atlantic Ocean.

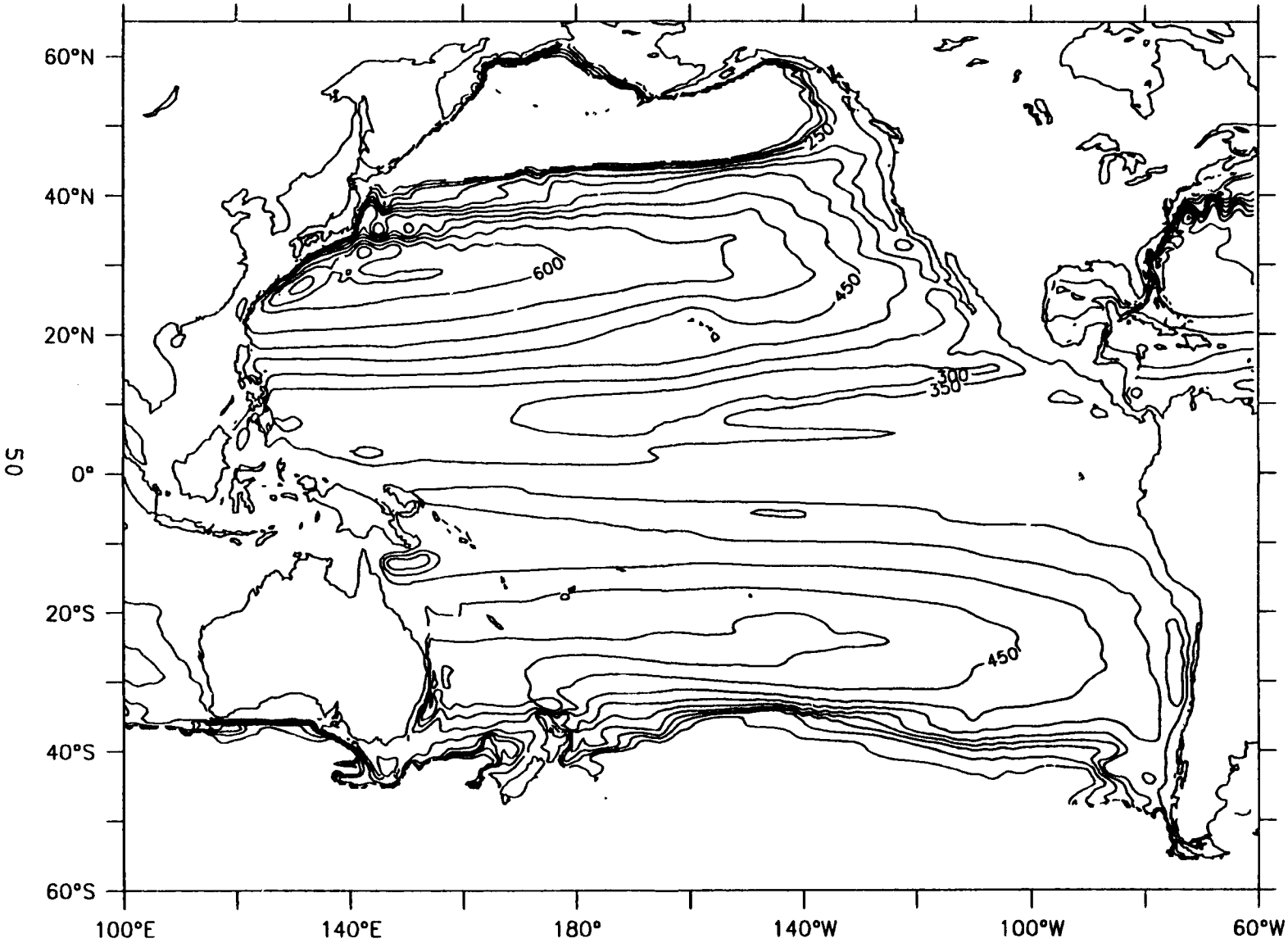

Figure 15. Depth in meters of the σ_θ = 26.5 surface (Layer B), Pacific Ocean.

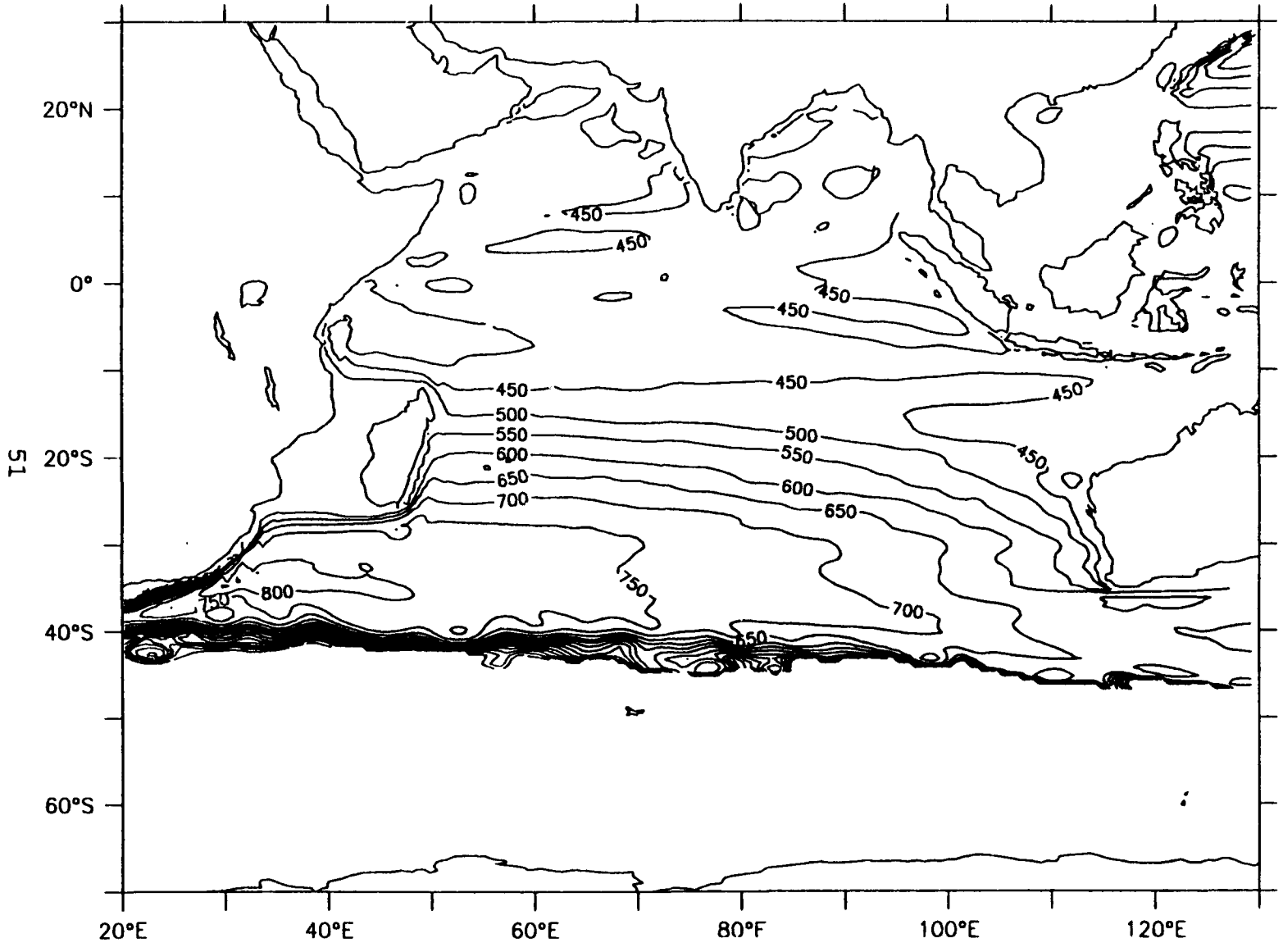

Figure 16. Depth in meters of the σ_θ = 26.75 surface (Layer B), Indian Ocean.

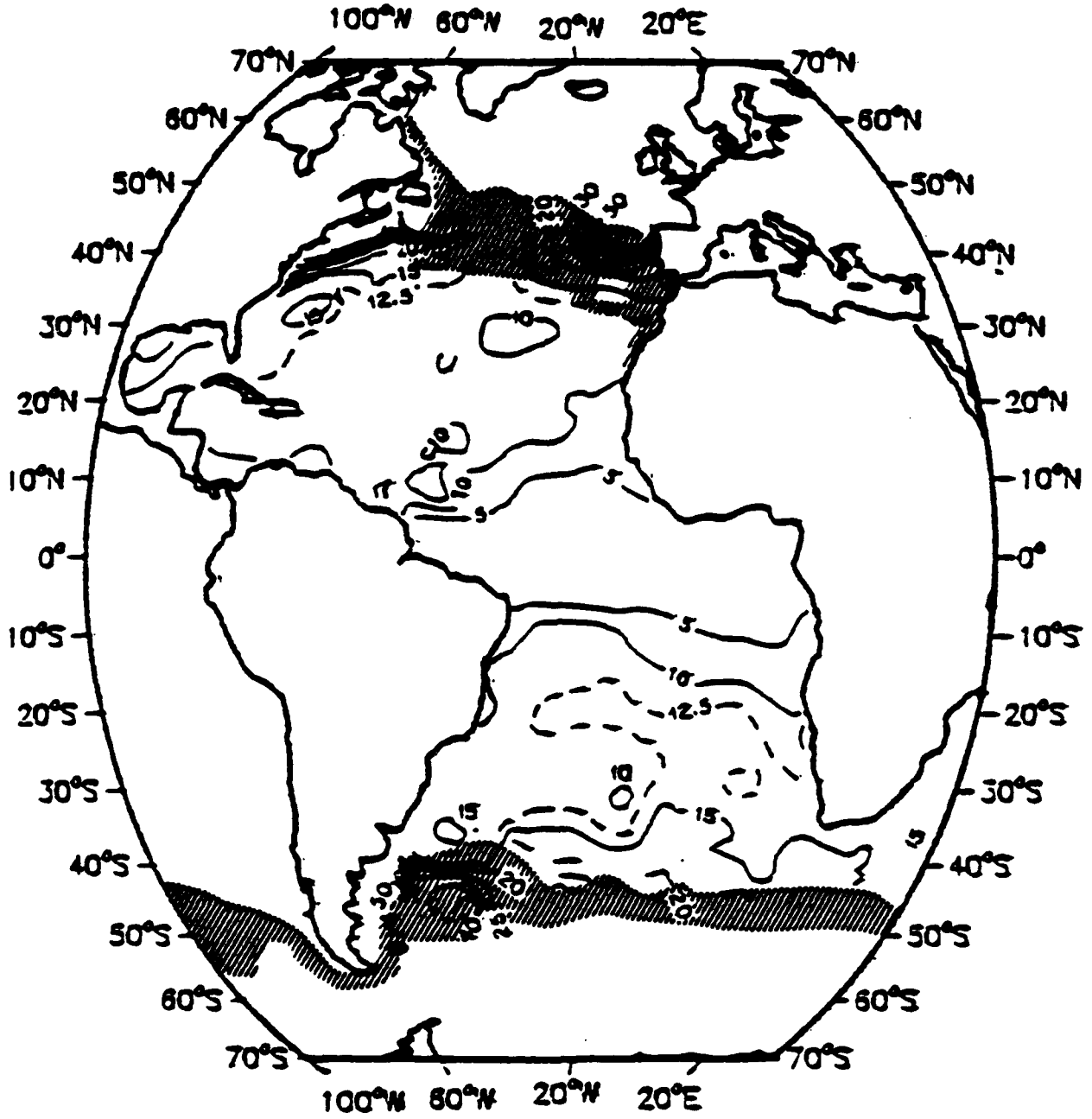

Figure 17. Potential vorticity of the σ_θ = 26.5-27.0 interval (Layer B), Atlantic Ocean. Other features as in Figure 11. Note the regions of homogenized potential vorticity in the North and South Atlantic (From Keffer, 1985).

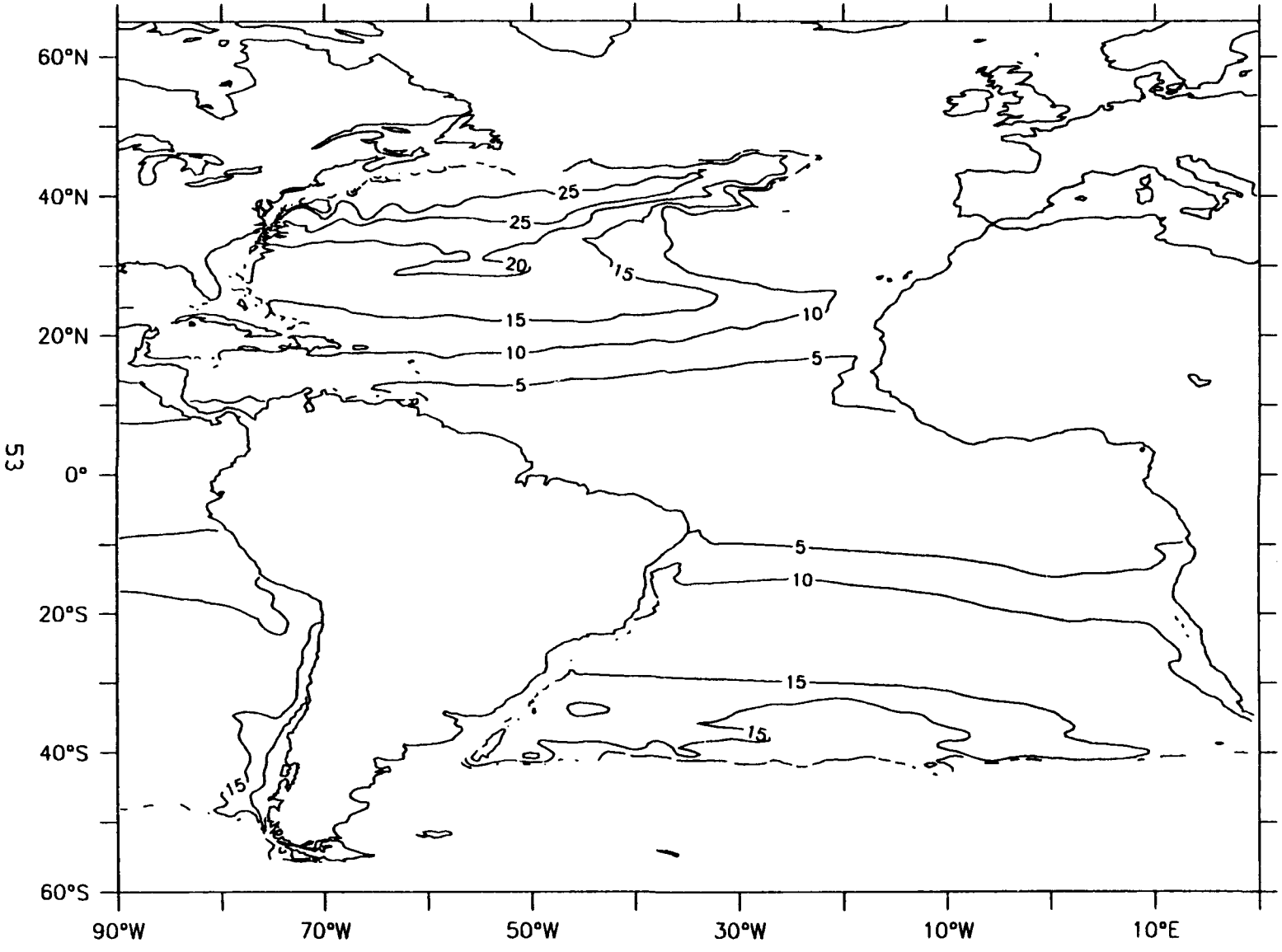

Figure 18. Potential vorticity of the σ_θ = 26.5-27.0 interval (Layer B), Atlantic Ocean.

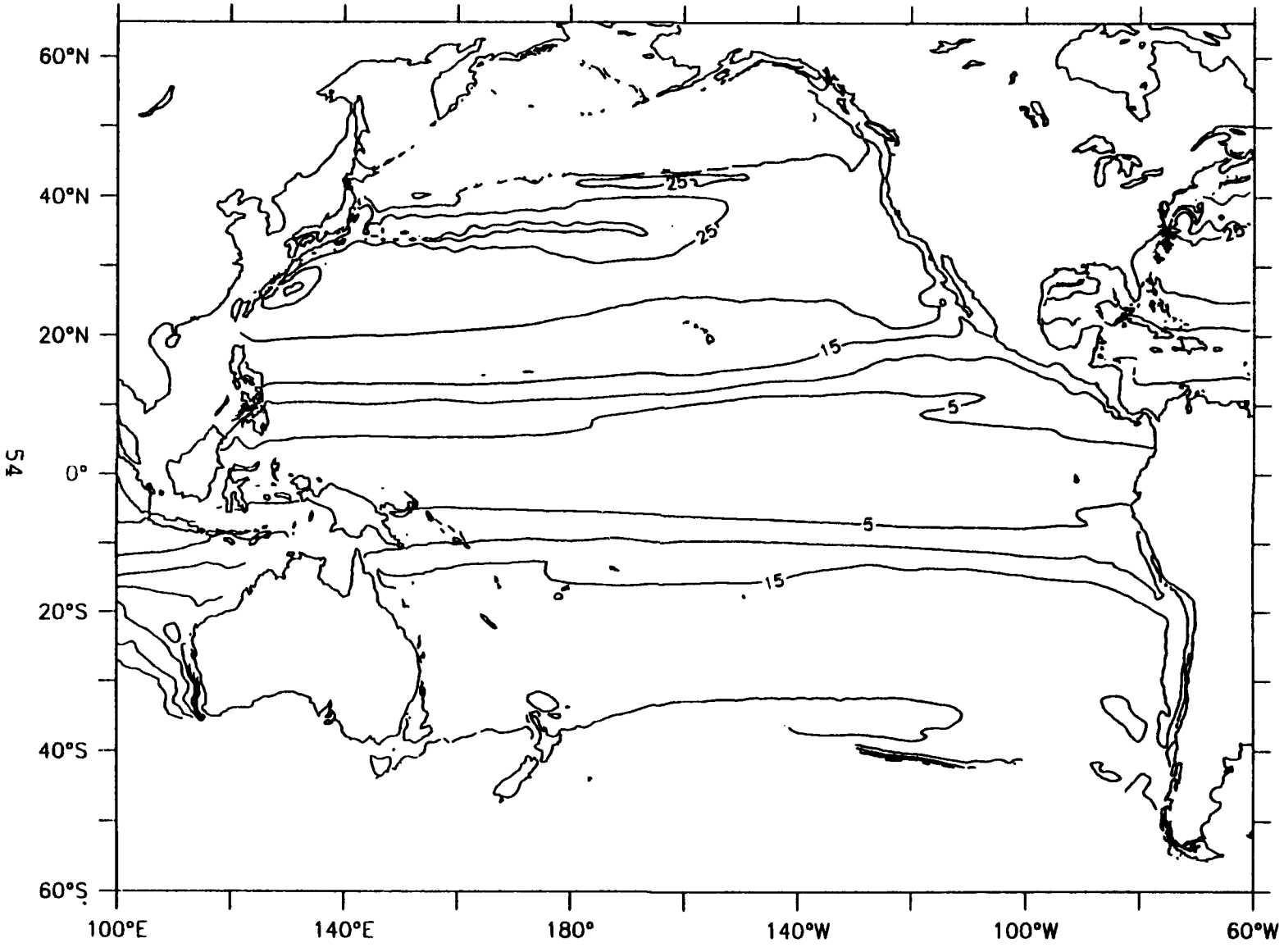

Figure 19. Potential vorticity of the σ_θ = 26.25-26.75 interval (Layer B), Pacific Ocean.

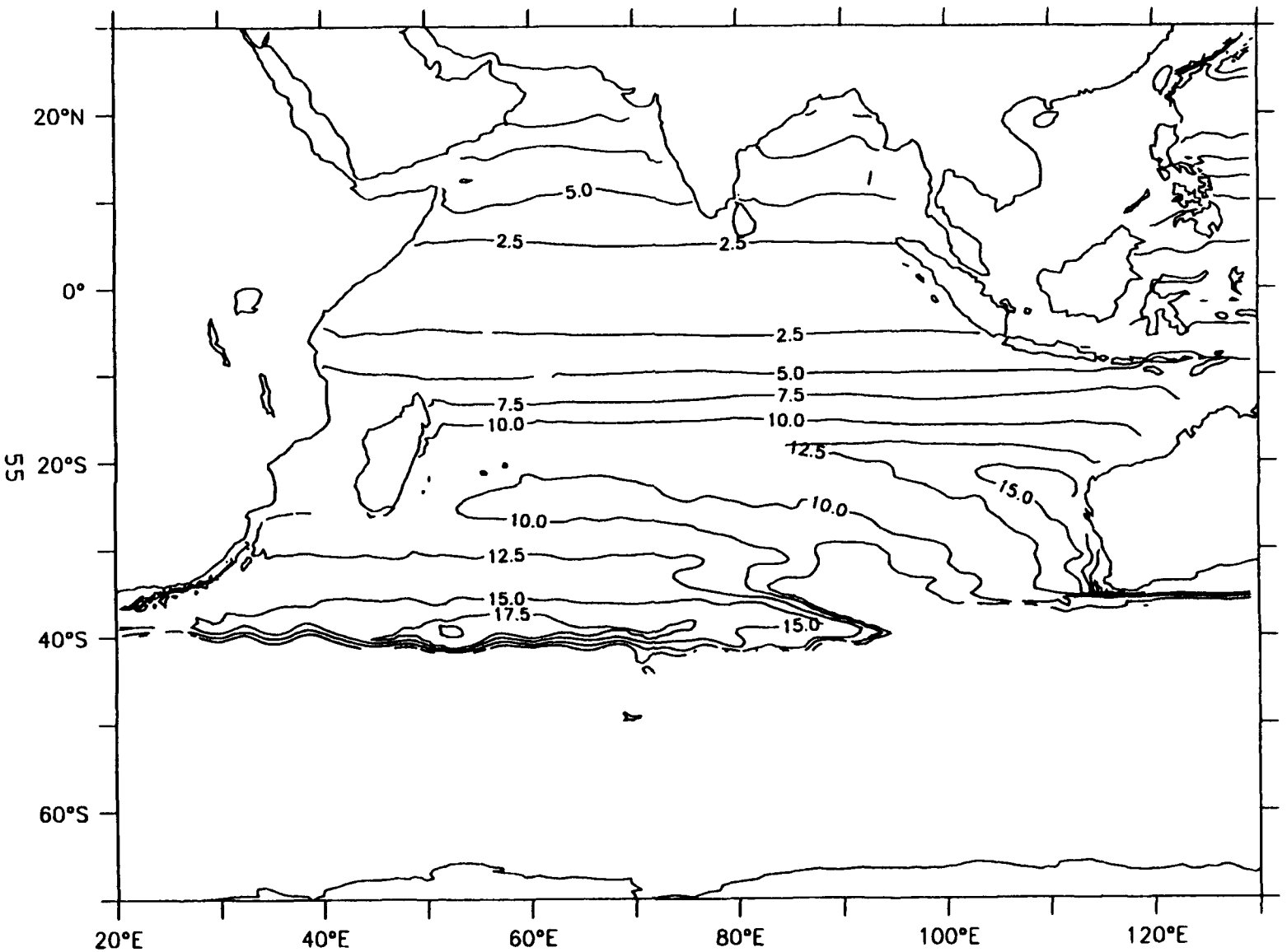

Figure 20. Potential vorticity of the σ_θ = 26.5-27.0 interval (Layer B), Indian Ocean.

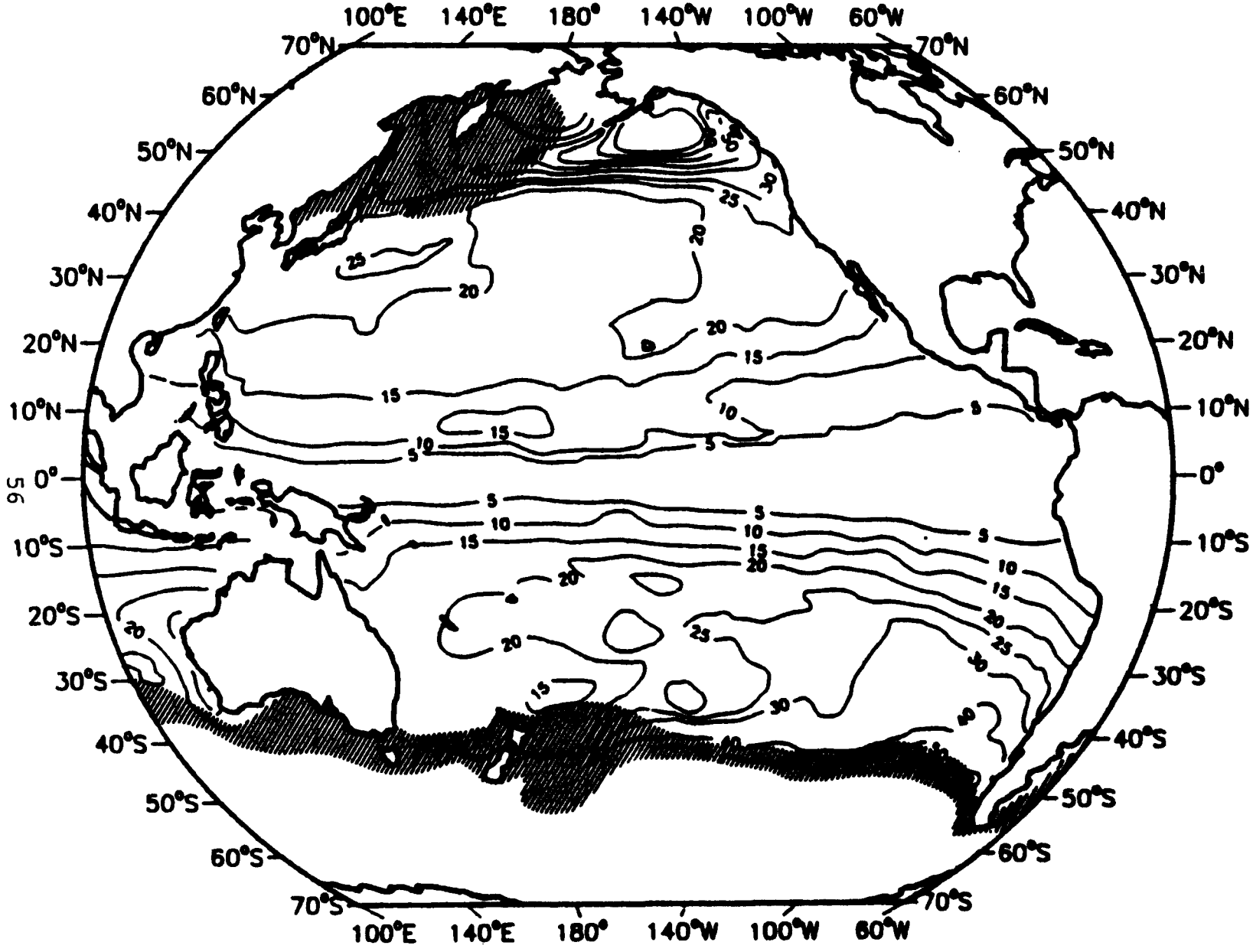

Figure 21. Potential vorticity of the σ_θ = 26.25-26.75 interval (Layer B), Pacific Ocean. Other features as in Figure 11. Note that while the subpolar and subtropical gyres of the North Pacific are homogenized, there is a sharp contrast of q between them (From Keffer, 1985).

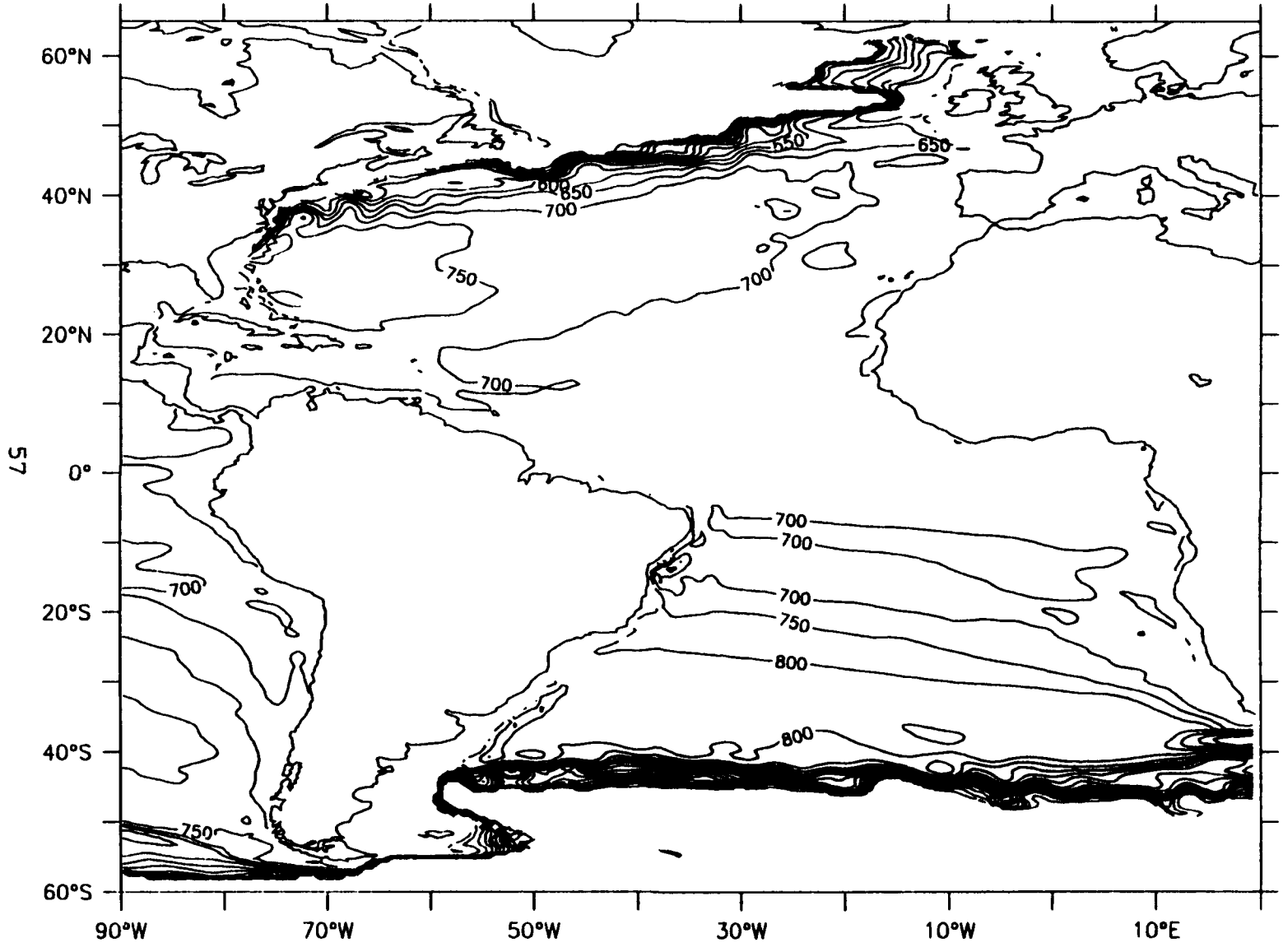

Figure 22. Depth in meters of the σ_θ = 27.15 surface (Layer C), Atlantic Ocean.

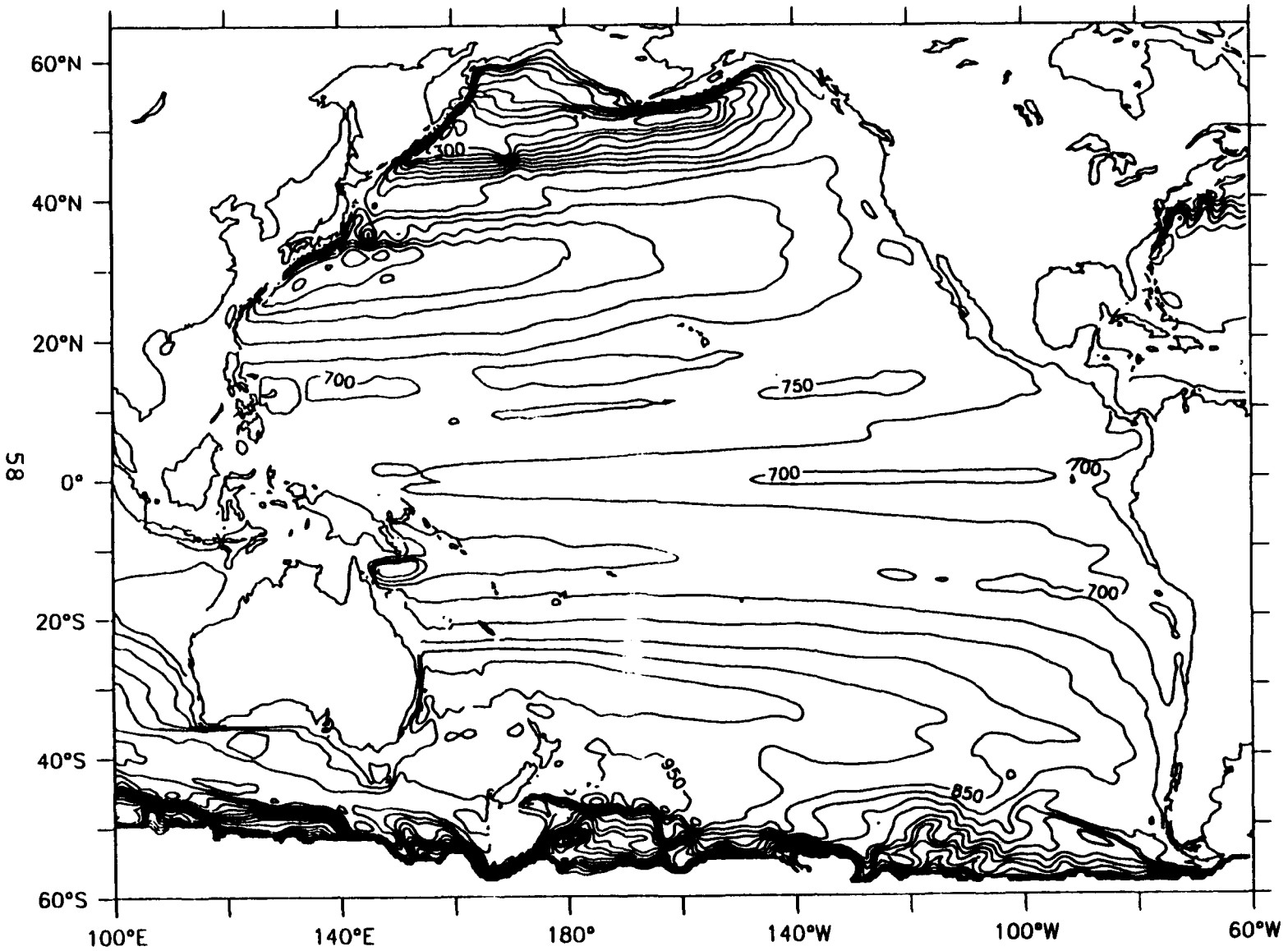

Figure 23. Depth in meters of the σ_θ = 27.15 surface (Layer C), Pacific Ocean.

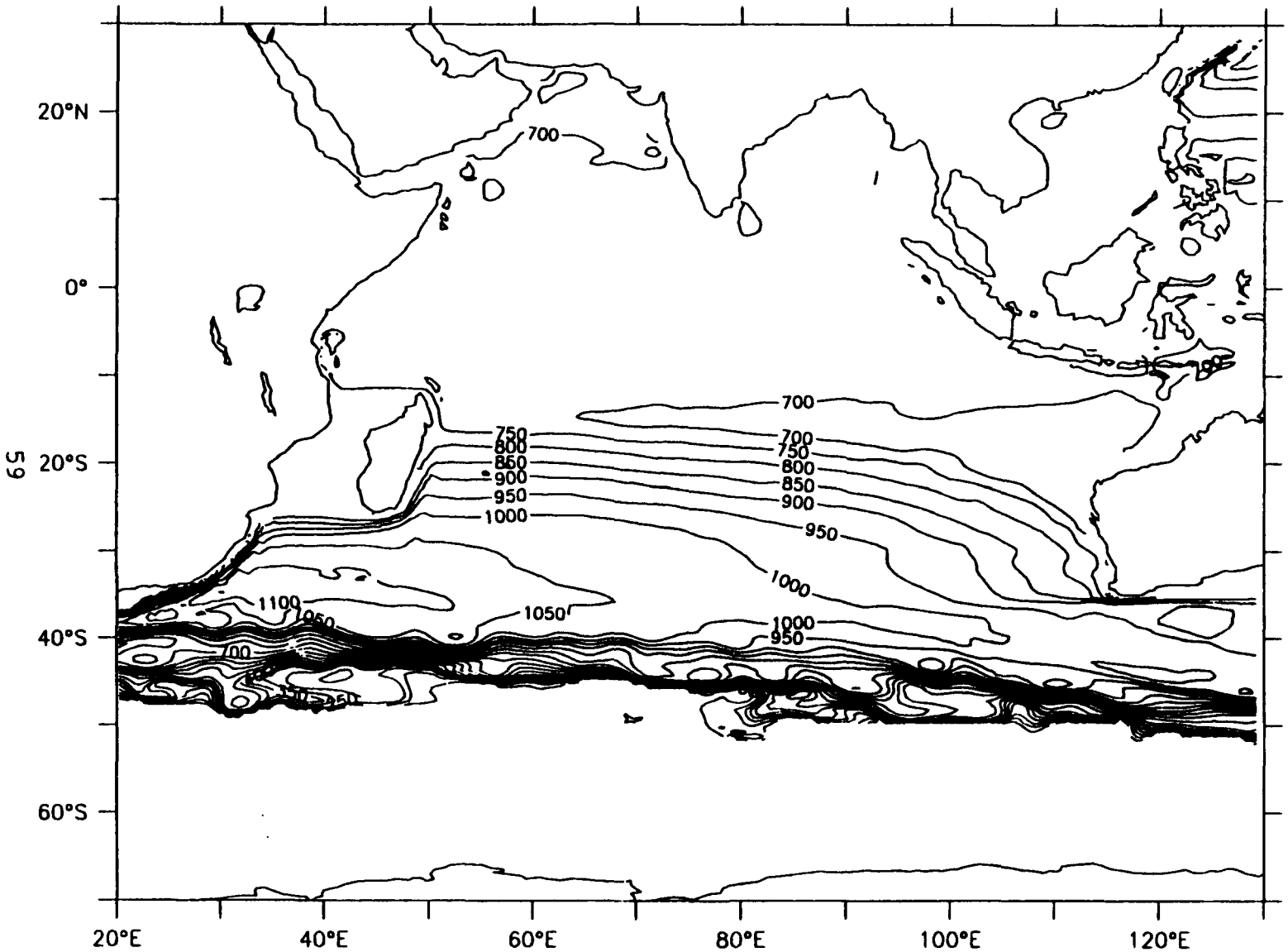

Figure 24. Depth in meters of the σ_θ = 27.15 surface (Layer C), Indian Ocean.

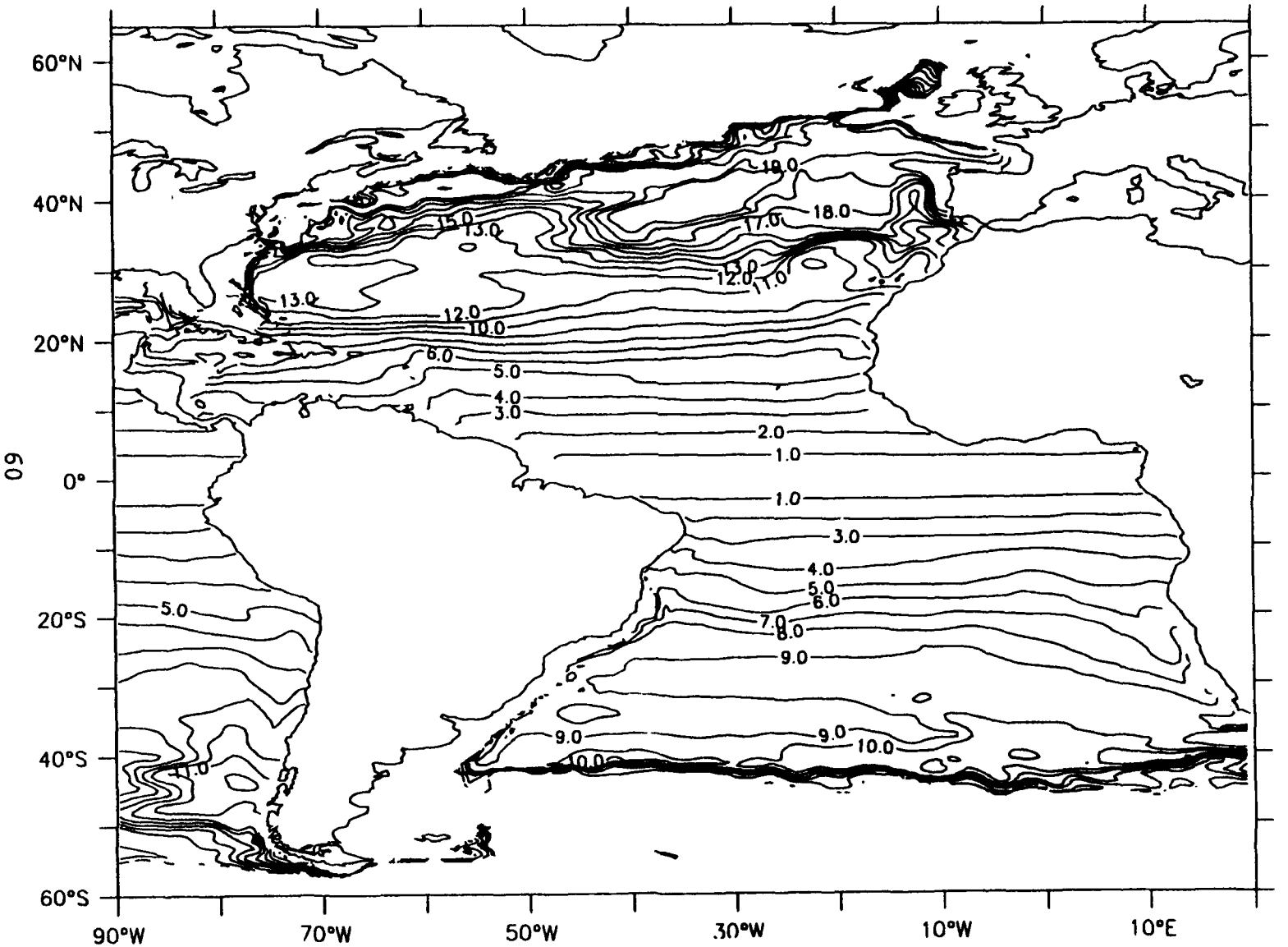

Figure 25. Potential vorticity of the σ_θ = 27.0-27.3 interval (Layer C), Atlantic Ocean.

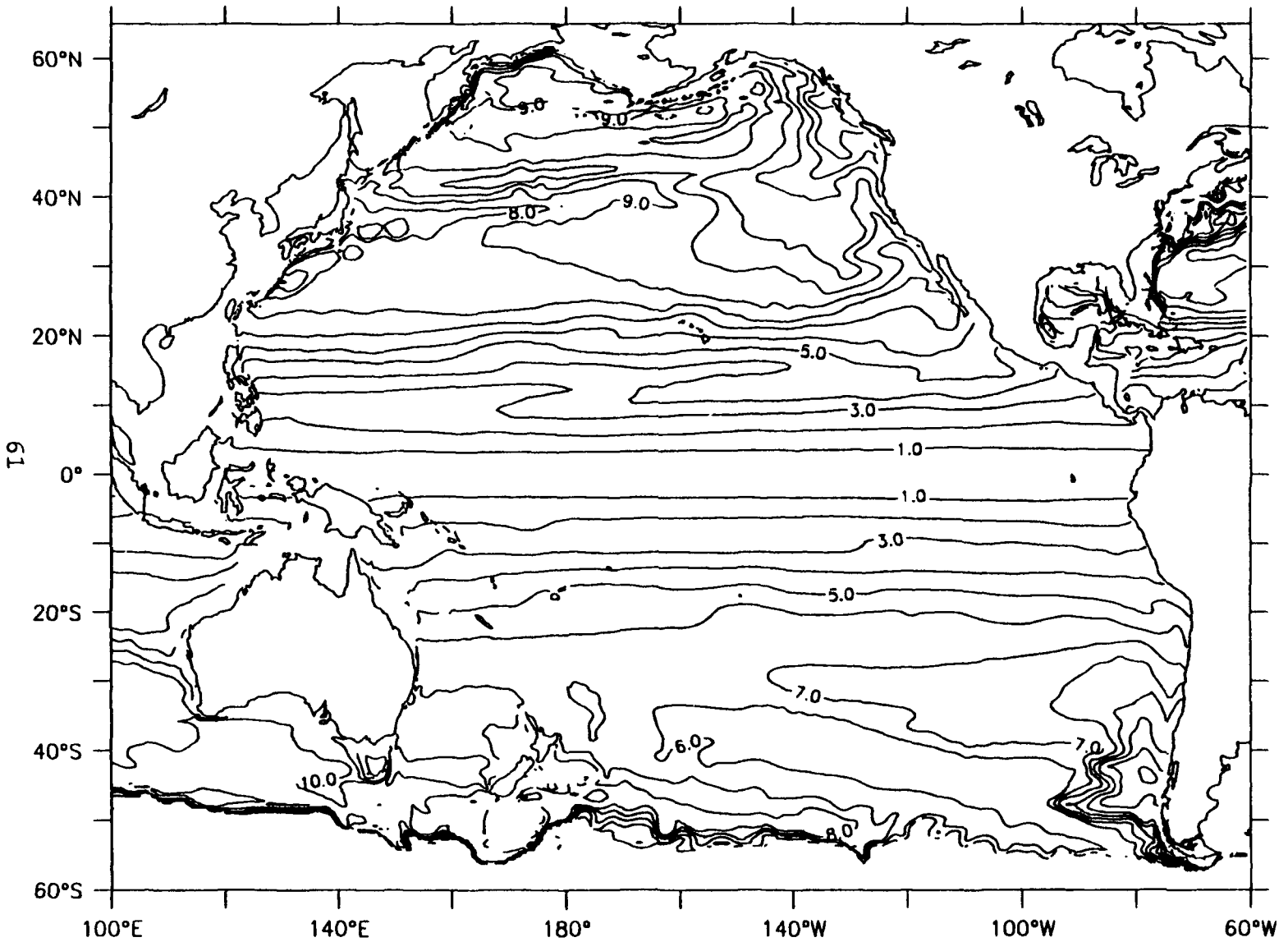

Figure 26. Potential vorticity of the σ_θ = 27.0-27.3 interval (Layer C), Pacific Ocean.

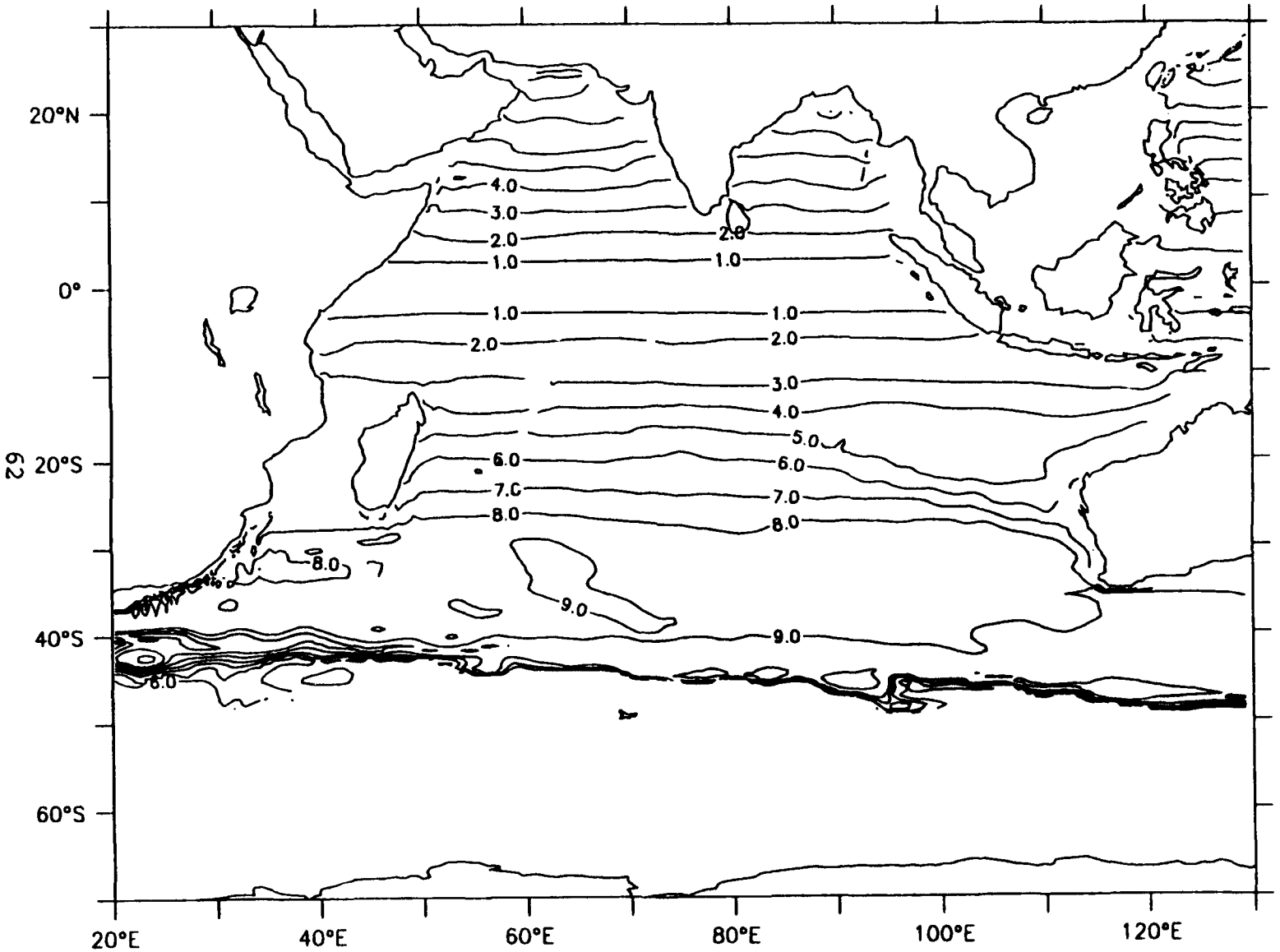

Figure 27. Potential vorticity of the σ_θ = 27.0-27.3 interval (Layer C), Indian Ocean.

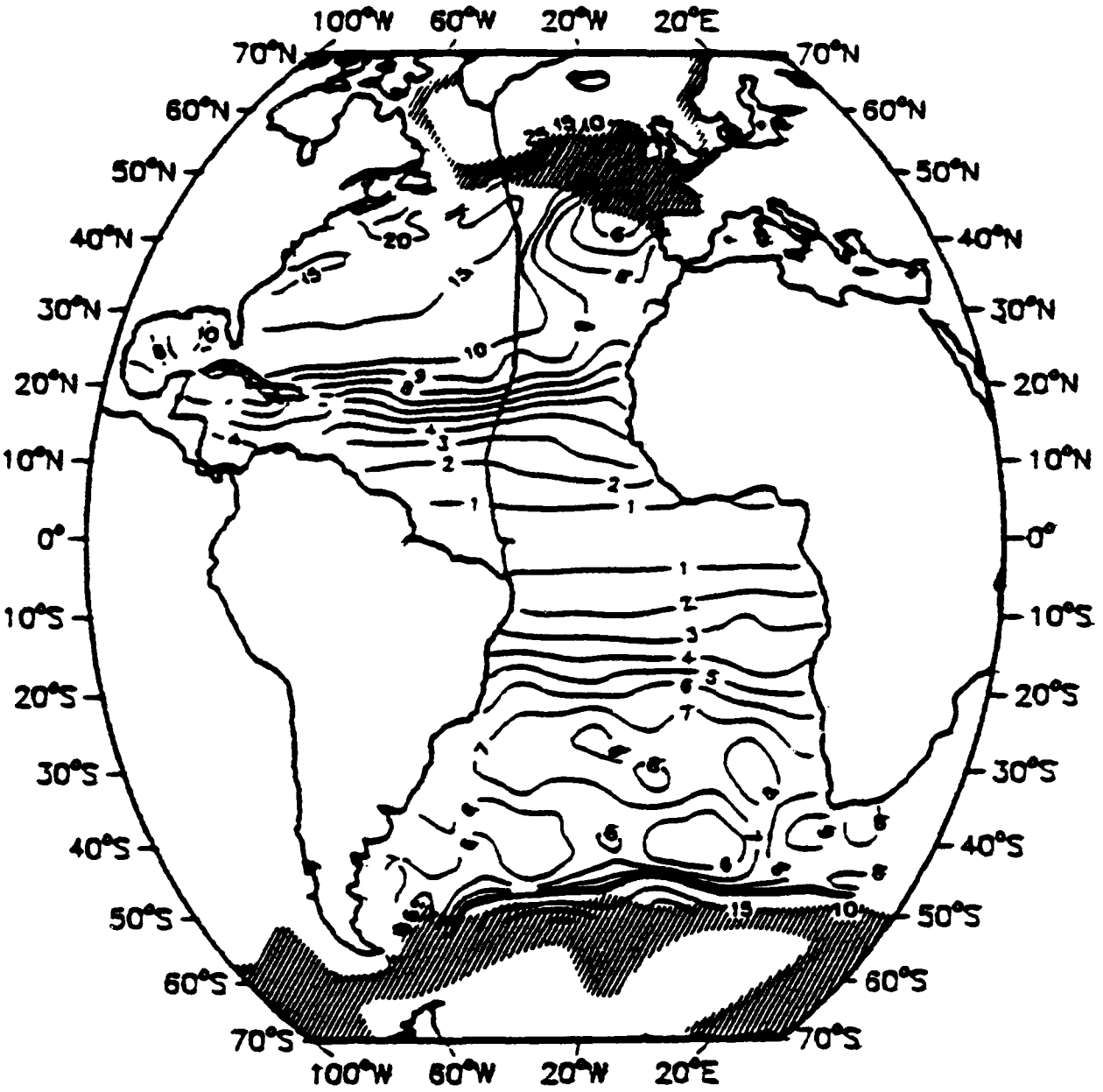

Figure 28. Potential vorticity of the σ_θ = 27.0-27.3 interval (Layer C), Atlantic Ocean. Other features as in Figure 11. Note the intrusion of low q water into the northeastern North Atlantic. This is the recirculation of subpolar mode water described by McCartney (1982) (From Keffer, 1985).

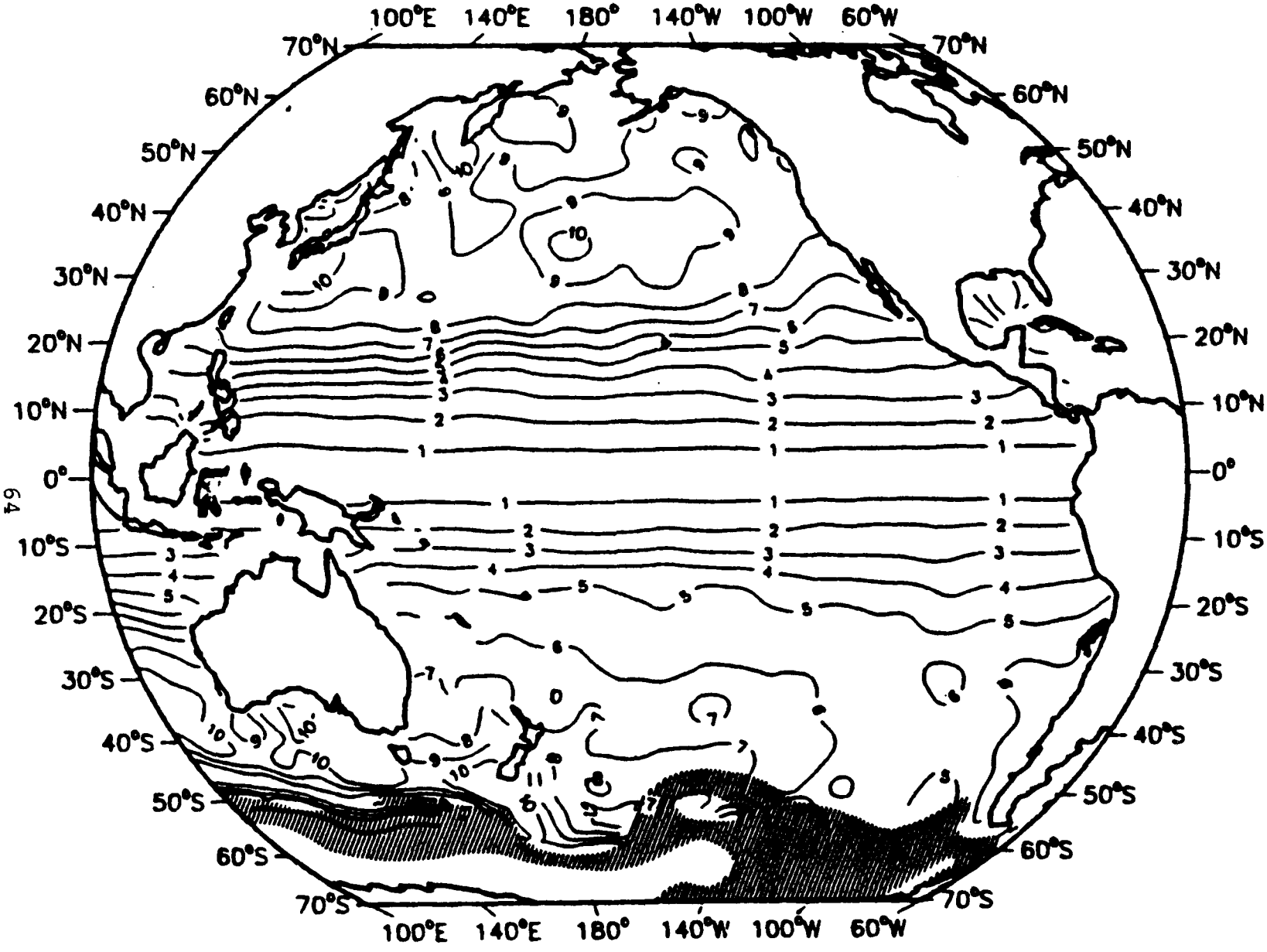

Figure 29. Potential vorticity of the σ_θ = 27.0-27.3 interval (Layer C), Pacific Ocean. Other features as in Figure 11. Note that within this interval, the contrast of q between gyres is one. The entire northern North Pacific has equilibriated to one value of q (From Keffer, 1985).

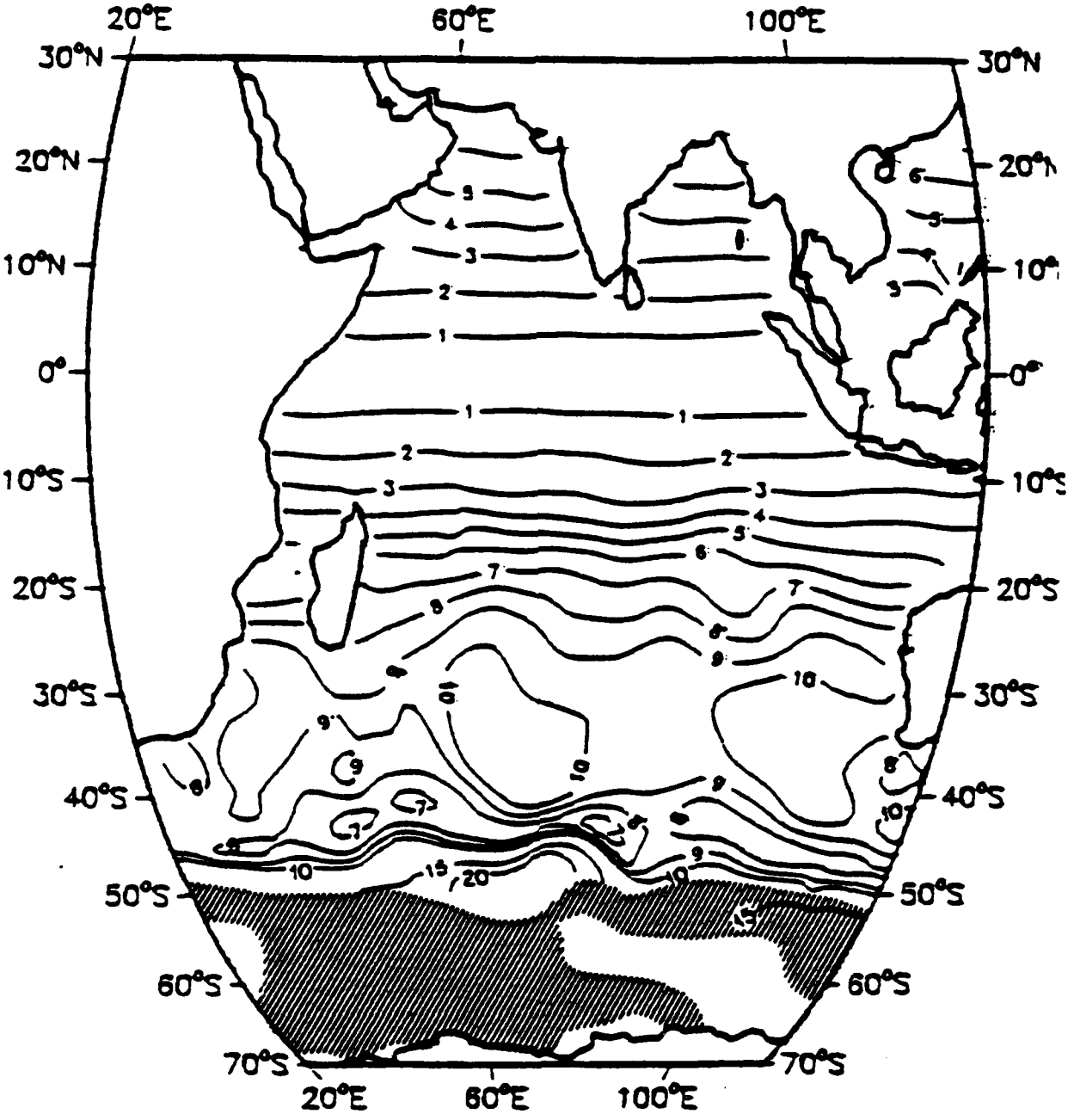

Figure 30. Potential vorticity of the σ_θ = 27.0-27.3 interval (Layer C), Indian Ocean. Other features as in Figure 11 (From Keffer, 1985).

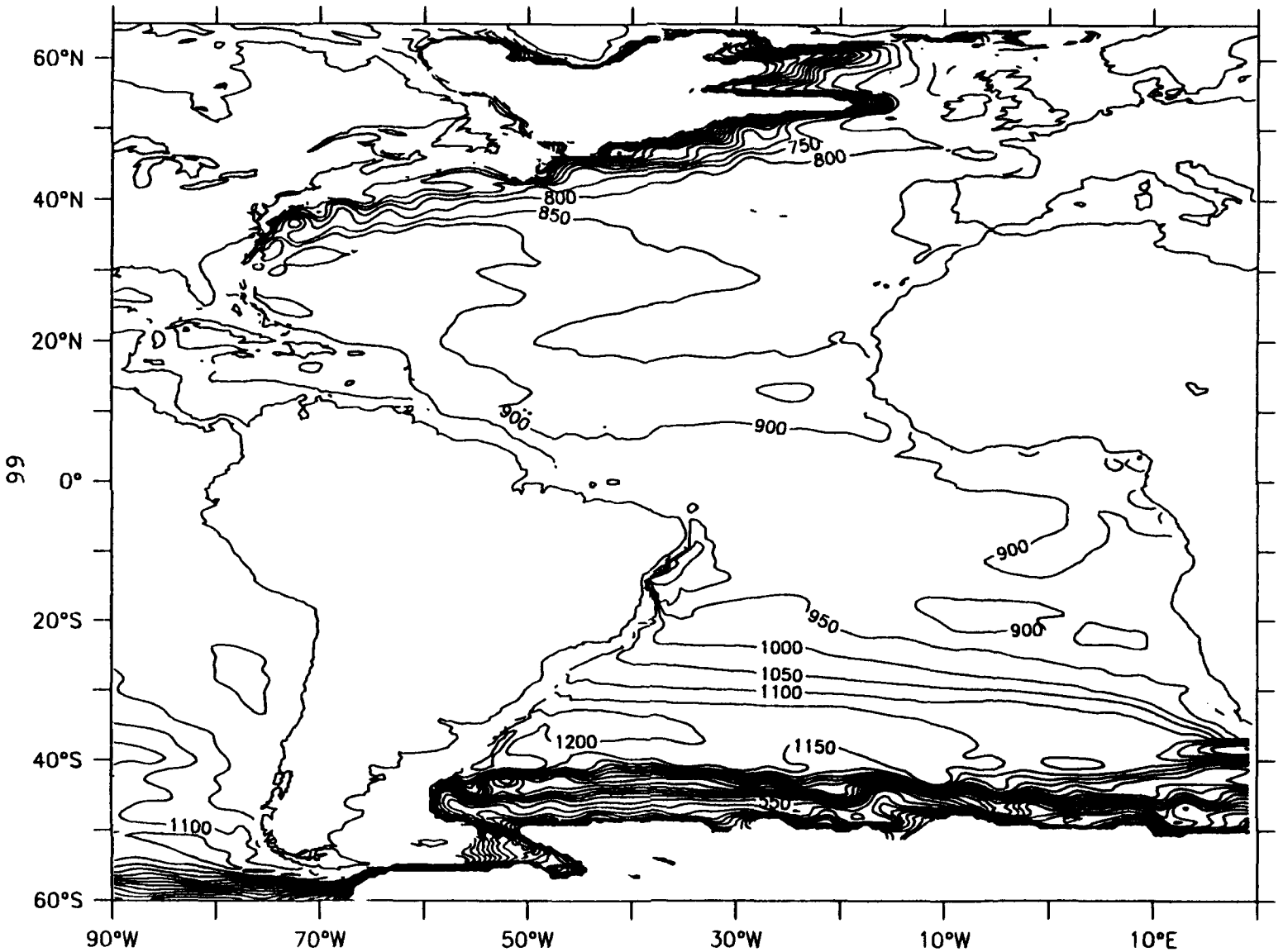

Figure 31. Depth in meters of the σ_θ = 27.4 surface (Layer D), Atlantic Ocean.

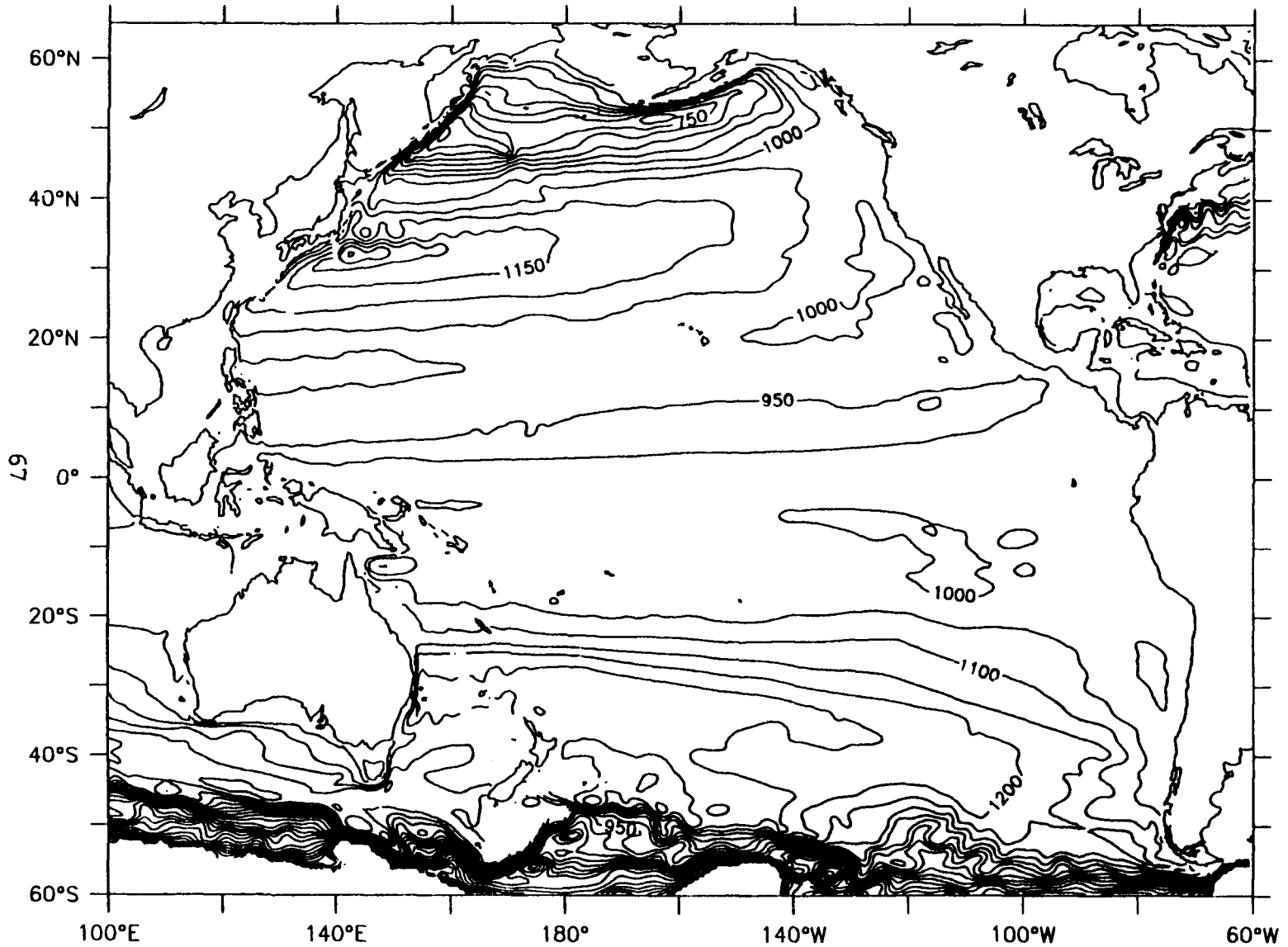

Figure 32. Depth in meters of the σ_θ = 27.4 surface (Layer D), Pacific Ocean.

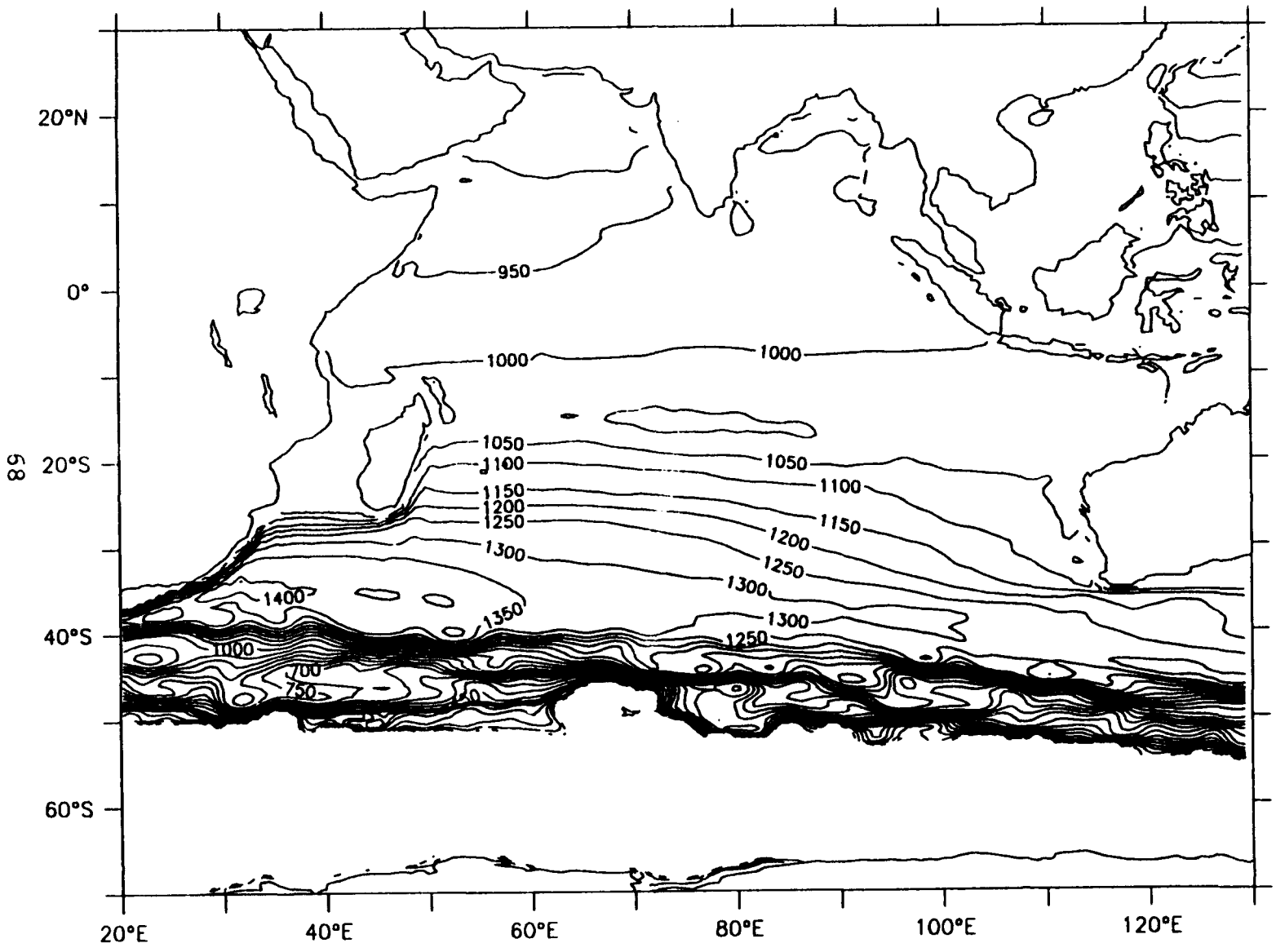

Figure 33. Depth in meters of the σ_θ = 27.4 surface (Layer D), Indian Ocean.

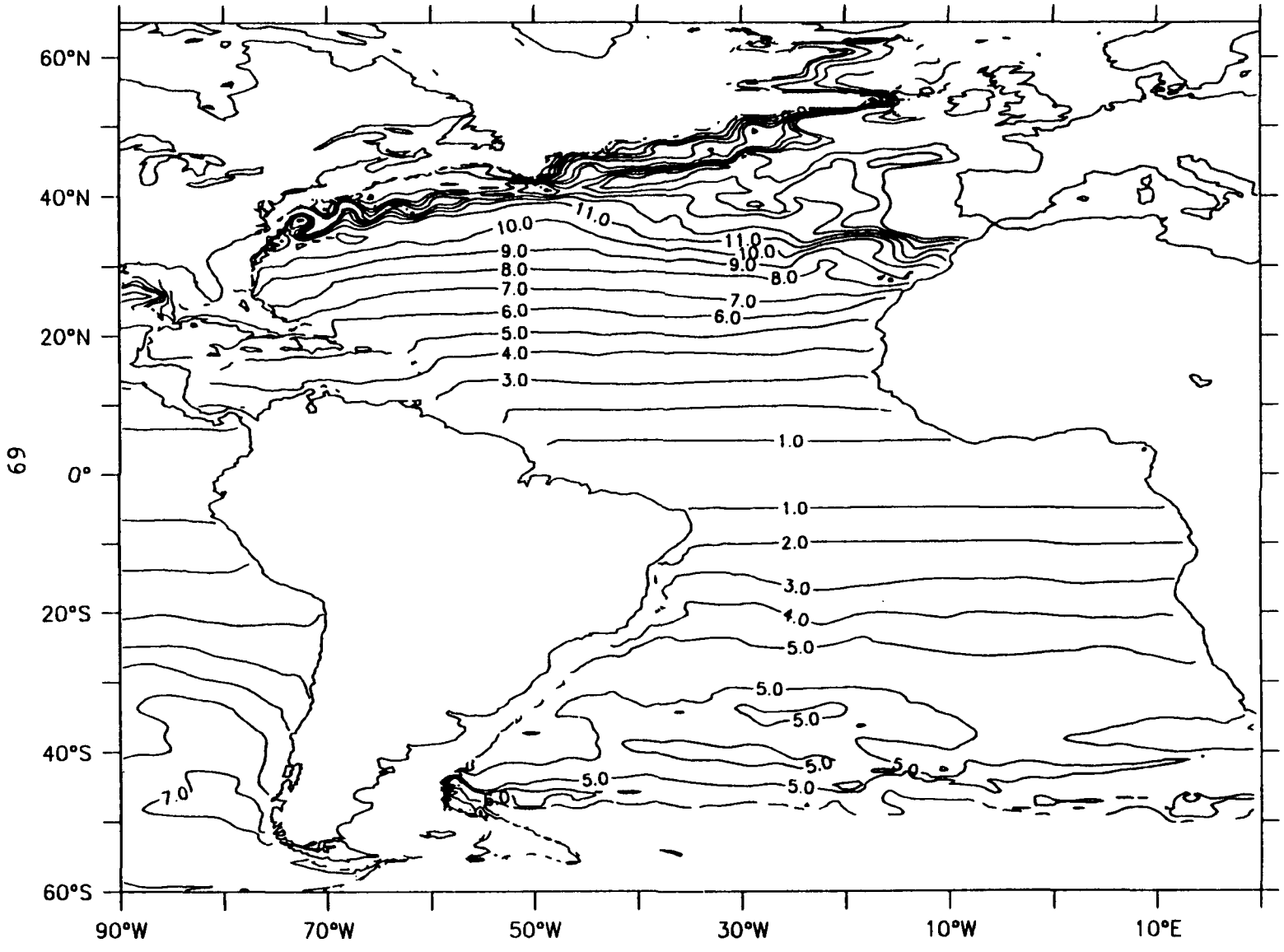

Figure 34. Potential vorticity of the σ_θ = 27.3-27.5 interval (Layer D), Atlantic Ocean.

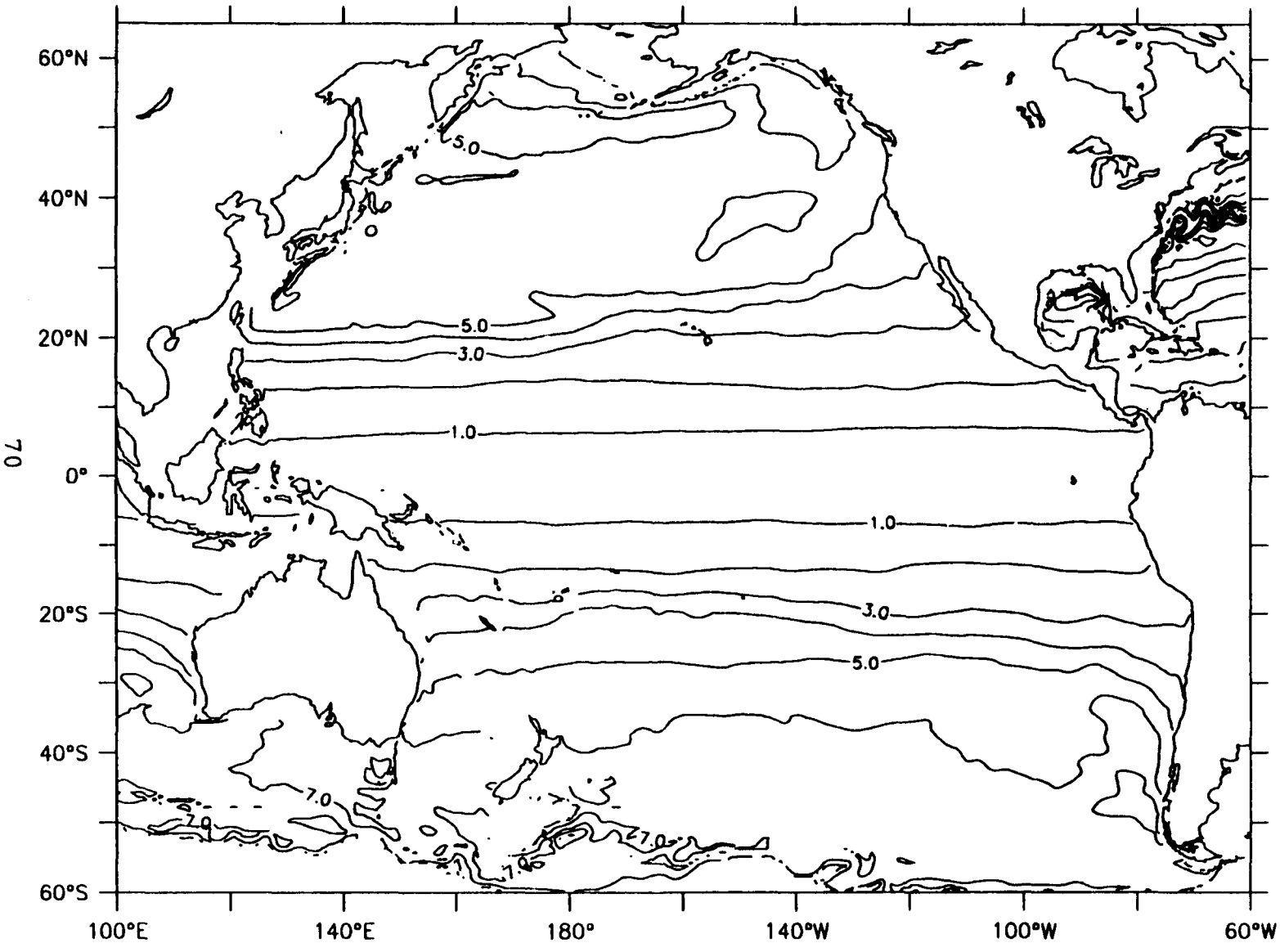

Figure 35. Potential vorticity of the σ_θ = 27.3-27.5 interval (Layer D), Pacific Ocean.

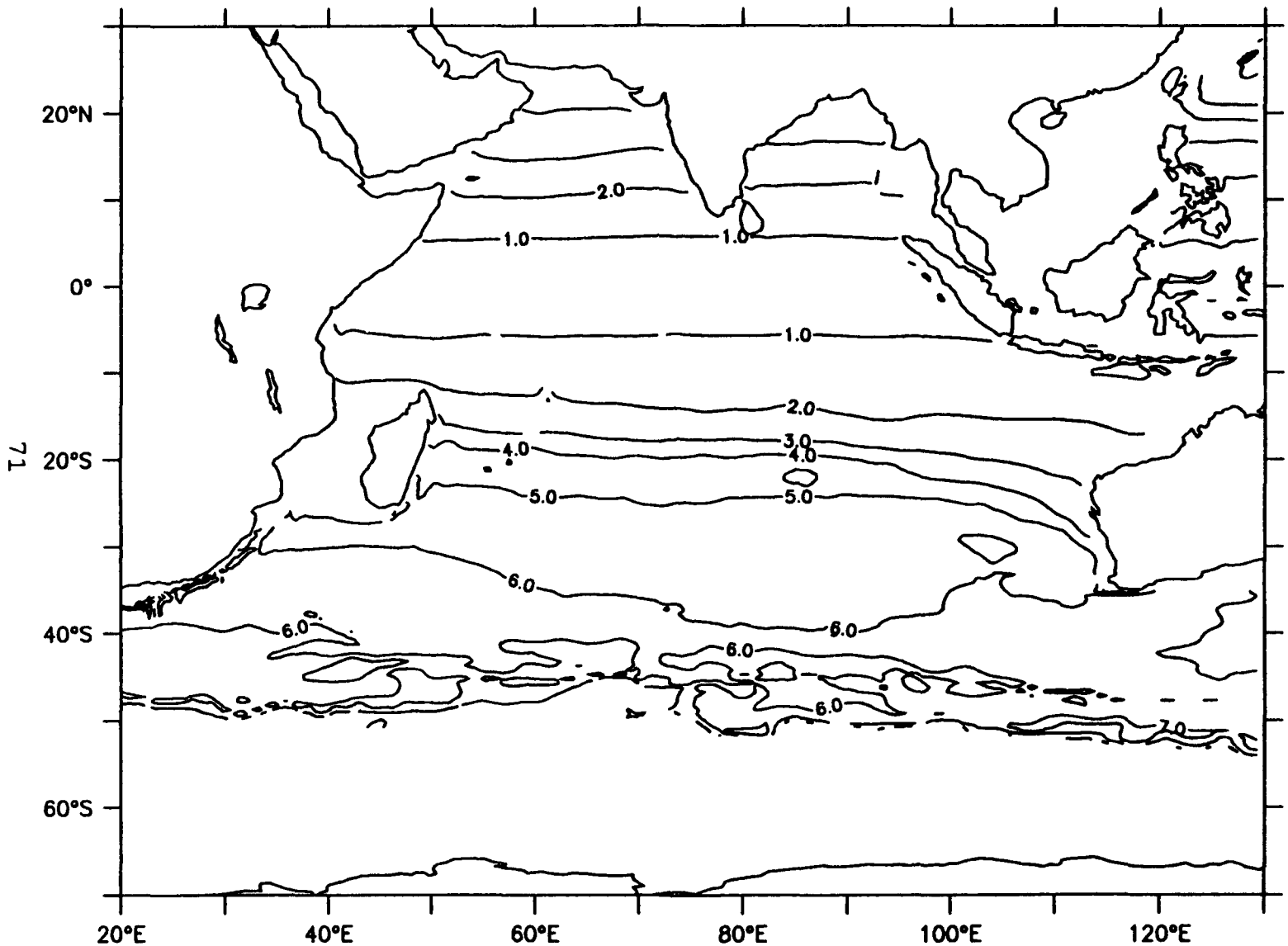

Figure 36. Potential vorticity of the σ_θ = 27.3-27.5 interval (Layer D), Indian Ocean.

Figure 37. Potential vorticity of the σ_θ = 27.3-27.5 interval (Layer D), Atlantic Ocean. The heavy dashed line in the North Atlantic is the line of zero wind stress curl. Other features as in Figure 11. Note that in the North Atlantic there is a tendency for the q contours to run from deep in the subtropical gyre into the outcrop region. This facilitates the replacement of Norwegian Sea overflow water (From Keffer, 1985).

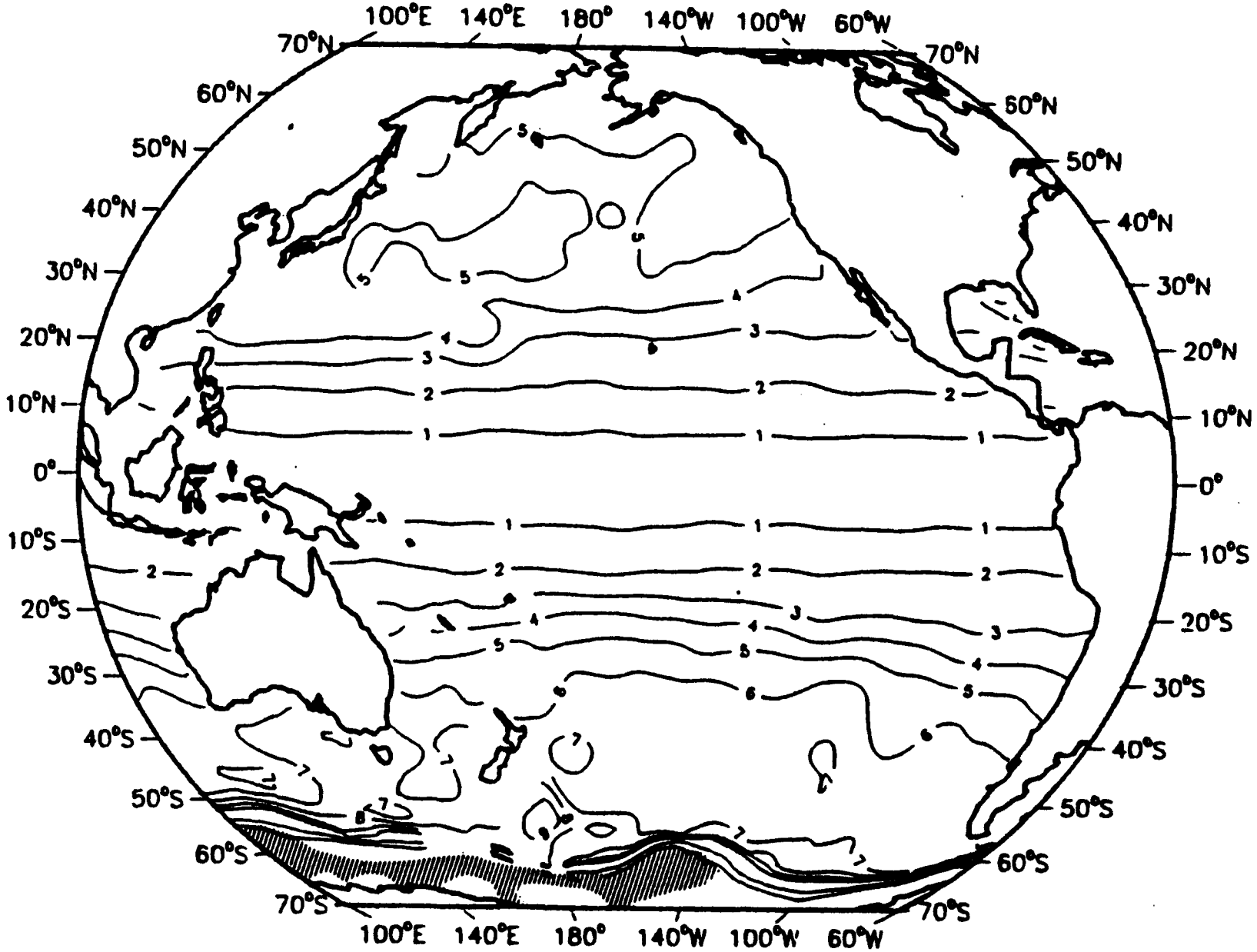

Figure 38. Potential vorticity of the σ_θ = 27.3-27.5 interval (Layer D), Pacific Ocean. Other features as in Figure 11. Note that both the North and South Pacific remain homogenized, even at great depth (From Keffer, 1985).

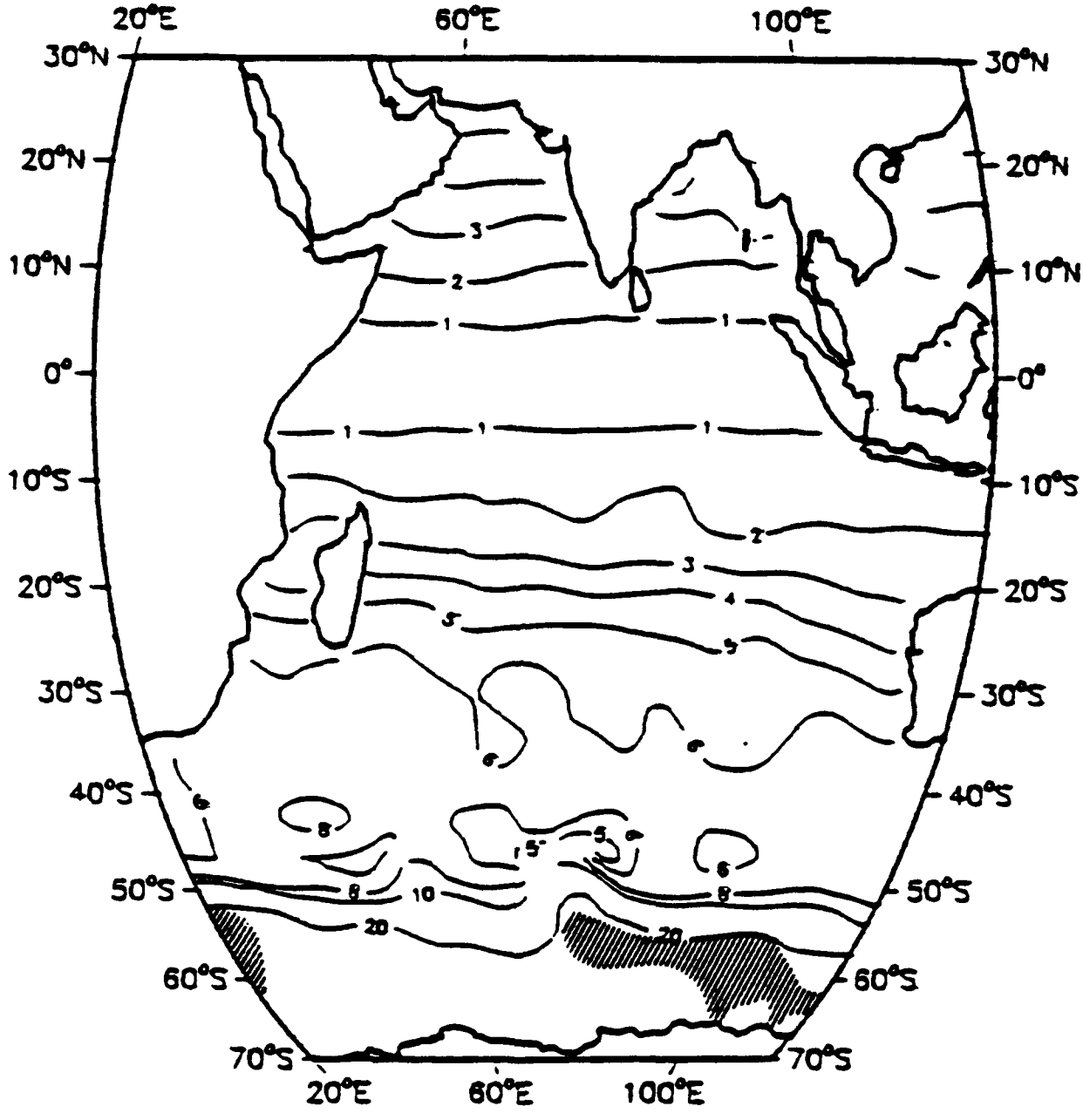

Figure 39. Potential vorticity of the σ_θ = 27.3-27.5 interval (Layer D), Indian Ocean. Other features as in Figure 11. Note that q is still largely homogenized (From Keffer, 1985).

INITIAL DISTRIBUTION LIST

1.	Defense Technical Information Center Cameron Station Alexandria, VA 22304-6145	2
2.	Library, Code 0142 Naval Postgraduate School Monterey, CA 93943-5002	2
3.	Chairman (Code OC/CO) Department of Oceanography Naval Postgraduate School Monterey, CA 93943-5000	1
4.	Chairman (Code MR/RD) Department of Meteorology Naval Postgraduate School Monterey, CA 93943-5000	1
5.	Albert J. Semtner Department of Oceanography Naval Postgraduate School Monterey, CA 93943-5000	1
6.	Mary L. Batteen Department of Oceanography Naval Postgraduate School Monterey, CA 93943-5000	1
7.	LT Douglas C. Marble 1310 Langston Drive Columbus, OH 43220	1
8.	Director Naval Oceanography Division Naval Observatory 34th and Massachusetts Avenue NW Washington, DC 20390	1
9.	Commander Naval Oceanography Command Stennis Space Ctr, MS 39529-5000	1
10.	Commanding Officer Naval Oceanographic Office Stennis Space Ctr Bay St. Louis, MS 39522-5001	1
12.	Library Scripps Institution of Oceanography P. O. Box 2367 La Jolla, CA 92037	1

13. Library 1
Department of Oceanography
University of Washington
Seattle, WA 98105

14. Library Acquisitions 1
National Center for Atmospheric Research
P.O. Box 3000
Boulder, CO 80307